NOMA in Cooperative Communication Systems with Energy-Harvesting Nodes and Wireless Secure Transmission

Abdelhamid Salem, *Member, IEEE*, and Leila Musavian, *Member IEEE.*

***Abstract*—In this paper, non-orthogonal multiple access (NOMA) in cooperative relay system is considered, where a source node communicates with a pair of energy harvesting (EH) user equipments through a multiple antennas relay node. A hybrid protocol is adopted at the relay, in which if the relay can successfully decode the signals, decode-and-forward (DF) protocol will be adopted to forward the signals to the users. Otherwise, amplify-and-forward (AF) protocol will be implemented. Assuming that the users adopt maximal ratio combining (MRC) to combine the received signals in the two cooperative phases, new explicit analytical expressions for the average sum-rate are derived when the relay works in, 1) AF mode, and 2) DF mode, in two scenarios when one user is the stronger in both cooperation phases, and when an alternative user is stronger in each phase. Then, the investigation is extended to the case where the relay is an untrusted node, and cooperative jamming technique is proposed to degrade the ability of the relay to decode the signals and enforce the relay to operate always in AF mode. For the untrusted relay scenario, new analytical expression for the average secrecy rate is derived. Monte Carlo simulations are provided to validate the analysis. The simulation results reveal that the location of the relay is the key parameter to achieve the best performance.**

***Index Terms*—NOMA, cooperative communications, energy harvesting, secrecy rate, physical layer security.**

I. Introduction

Non-orthogonal multiple access (NOMA) technique has received significant attention as a viable multiple access technique for fifth Generation (5G) mobile communication networks. NOMA provides an effective solution to enhance the spectral efficiency of the communication networks [1]. The main idea of NOMA is to realize multiple access in power domain which differs from the conventional orthogonal multiple access (OMA) techniques. In down-link, the source superimposes the signals of the users in the same time, frequency, and code domains, however in different power domains. The user signal decoding is then based on successive interference cancellation (SIC). Thus, NOMA can potentially consume the spectrum more efficiently, compared to OMA, by opportunistically exploring multiple users' channel conditions [1], [2]. Consequently, achievable sum-rate in NOMA can be significantly enhanced compared with that of the conventional OMA techniques in favorable circumstances. In this direction, the performance of a down-link NOMA was investigated in [2], which showed that NOMA can achieve superior performance in terms of sum-rate comparing with the OMA schemes. In [3], optimal power allocation to maximize fairness among users of a NOMA down-link system was investigated. The performance of a down-link NOMA was evaluated assuming that the channel state information (CSI) is available at the transmitter in [4]. On the other hand, the impact of user pairing on the performance of a NOMA system was explored in [5], which showed that the performance gain achieved by NOMA over conventional OMA can be enhanced by selecting users whose channel conditions are more distinctive. Moreover, combining NOMA and cooperative transmission communications can further enhance the spectral efficiency. In this regard, NOMA in a coordinated direct and relay transmission was considered in [6], where a transmitter communicates directly with the first user, while communication with the second user is provided only through a relay node. It was shown that the proposed NOMA in coordinated direct and relay transmission can provide remarkable performance gain compared to NOMA in non-coordinated transmission [6]. NOMA in multiple-antenna relaying systems using maximal ratio combining (MRC) at the receiver is considered in [7] which assumed that the transmit antenna at the relay that maximizes the signal-to-noise ratio (SNR) was selected for relaying the signal; simulation results of this work have clearly shown the superiority of NOMA over OMA. Cooperative relaying system using NOMA to improve the spectral efficiency considering the achievable average rate was analyzed for independent Rayleigh fading channels in [8]. The exact expression of the average achievable rate of NOMA-based cooperative relaying systems for Rician fading channels was derived in [9]. The application of simultaneous wireless information and power transfer (SWIPT) to NOMA systems was investigated in [10], which proposed a new cooperative SWIPT NOMA protocol, in which the users who are close to the

A. Salem is with the Department of Electronic and Electrical Engineering, University College London, London WC1E 7JE, U.K. (e-mail: a.salem@ucl.ac.uk). L. Musavian is with the School of Computer Science and Electronic Engineering, University of Essex, Colchester, CO4 3SQ, UK. (e-mail: Leila.musavian@essex.ac.uk). This work is supported By the UK EPSRC under grant EP/N032268/1.

transmitter work as energy harvesting relays to help farther users. The outage performance of cooperative relaying transmissions in two-user NOMA networks, where SWIPT was adopted at the near users to recharge their batteries was studied in [11]. On the other hand, a cooperative NOMA network was considered in [12], which assumed a source communicates with two users via an energy harvesting relay node, and the impact of power allocation policy on the considered cooperative SWIPT system was analyzed. In [13] the effect of energy constraint on two-hop networks with random medium access was considered. The authors in [14] used an opportunistic multiple access protocol which monitors the priorities between the users to better use the limited energy resources.

Furthermore, due to the broadcast nature of wireless communication channels, providing security in wireless networks is challenging. For this purpose, the concept of physical layer security was first introduced by Wyner in [15] where it was shown that secret communication is possible if the eavesdropper channel is a degraded version of the destination channel. In this regard, several physical layer security techniques, such as cooperative jamming technique [16], [17], were proposed to enhance the system secrecy, even in cases where the eavesdropper has better channel condition than the legitimate receiver. In this context, in cooperative relaying systems, the relay might be an untrusted node and acts as both helper and eavesdropper at the same time. In such cases, the transmitted messages must remain secret even when the relay is used for transmission. In this respect, a coding technique was considered in [18] under the condition that some of the messages should be secret to the relay. Also, an achievable secrecy-rate for the general untrusted relay channel was provided in [19], [20]. Furthermore, using the destination as a jammer in the first time cooperation slot was proposed in [21], [22]. In general, these papers have shown that cooperation still can be beneficial for achieving secure communication.

In this paper, we consider NOMA in cooperative multiple antennas relaying systems, where the source and the relay both have fixed power supplies, whereas the users' equipments (U1 and U2) are energy harvesting nodes and adopt power splitting SWIPT technique to harvest the energy and process the information signals. We assume that the relay adopts a hybrid protocol which is when the received signal to interference noise ratio (SINR) at the relay is larger than a predefined threshold, i.e., the relay can successfully decode the signals, decode-and-forward (DF) protocol will be adopted to forward the signals to the users. Otherwise, amplify-and-forward (AF) protocol will be implemented. The users also adopt maximal ratio combining (MRC) to combine the received signals in the two phases. The exact analytical expressions of the average sum-rate are derived in different scenarios, 1) when the relay works in AF mode and a user is the stronger one in the two cooperation phases, 2) when the relay works in AF mode and different users are stronger in the two cooperation phases, 3) when the relay works in DF mode and a user is the stronger one in the two phases, and 4) when the relay works in DF mode and different users are stronger in the two phases. We then extend the investigation to the case where the relay is an untrusted node, and cooperative jamming technique is proposed to degrade the SINR at the relay and enforce it to work always in AF mode. For this scenario, explicit expression of the average secrecy rate is derived.

The performance analysis of cooperative NOMA systems when the relay is equipped with multiple antennas and the EH-users receive signals in the two phases is hard and challenging, since the users apply MRC and the overall signal to interference and noise ratios include two terms. In addition, in the untrusted relay scenario, the jamming power is a random variable and depends on the channel characteristics, which makes the performance analysis further challenging. The approaches developed in this paper can be extended to handle many general scenarios, for instance full duplex relaying, and multiple relays/users under certain conditions.

The major contributions of this paper are summarized below.

1) New analytical expressions for the average achievable rates of the proposed NOMA cooperative system when the hybrid relay is in AF mode are derived and presented over Rayleigh fading channels in two cases. Firstly, when the stronger user in the first cooperation phase is also the stronger user in the second cooperation phase. Secondly, when the stronger user in the first cooperation phase is the weaker user in the second phase.
2) The performance of the proposed NOMA cooperative system when the hybrid relay works in DF mode is analyzed and new explicit expressions for the average achievable rates over Rayleigh fading channels are derived also in two cases. The first case is when the stronger user in the first phase is the stronger one in the second phase. The second scenario is when the stronger user in the first phase is the weaker one in the second phase.
3) New analytical expression of the average secrecy rate is derived when the relay is an untrusted node and can act as an eavesdropper. In this case, we propose a cooperative jamming technique, in which the stronger user uses its harvested energy and works as a jammer to enforce the relay to work in AF mode.
4) Monte Carlo simulations are provided to confirm the analysis. Also, and the impacts of various system parameters on the adopted performance metrics are investigated.

The analytical results provided in this paper show that the good selection of the relay position is the key for achieving the best achievable sum and secrecy rates.

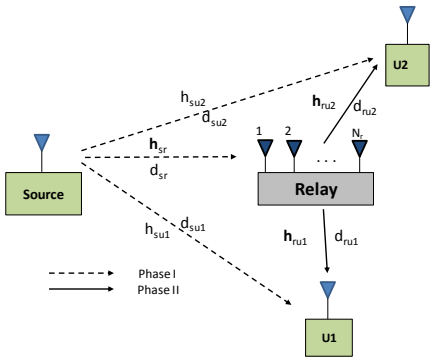

Figure 1: System model with multi-antenna relay and two users.

Also, increasing the signal to noise ratio (SNR) and the number of antennas at the relay node can enhance the performance of the proposed system.

This paper is organized as follows. In section II, we describe the system model. Sections III, and IV derive new analytical expressions for the average sum-rates of the AF,- and DF-based systems, respectively. In Section V, new analytical expressions are derived for the average secrecy rate when the relay is an untrusted node. Numerical examples and simulation results are presented and discussed in section VI. Finally, Section VII outlines the main conclusions of this work.

II. System Model

We consider a down-link NOMA cooperative communication system, in which a source node transmits information signals to energy constrained users with the help of a multiple antenna relay node, as shown in Fig.1. In NOMA systems, the stronger user adopt SIC technique to cancel out the interference (the weaker users' signals). However, when multiple users are admitted at the same time, the interference can be strong in cooperative NOMA systems. Due to the presence of this strong interference, the processing delay and complexity at users dramatically increase when the number of users grows. Therefore, in order to reduce the interference, processing delay and complexity, and to avoid the imperfect SIC, we consider a two users scenario, as also considered widely in literature including [23]. In addition, the insights of the two-user system model can be used to design user pairing schemes in a general cooperative NOMA system. In these scenarios, in order to decrease the complexity of message detection, a user pairing technique can be used to ensure that only two users share a specific orthogonal resource slot. User pairing technique can also be used in applications where there are two levels of users with multiple users in each group, and NOMA scheme is implemented among the users within each group [24]. We assume that, the source and relay both have fixed power supplies while the users, namely, U1 and U2, are EH nodes which solely rely on their RF harvested energy. Each user implements a power-splitting EH receiver to harvest energy and process information from the received observations. In addition, the source and users are equipped with a single antenna, while the relay is equipped with, N_r, antennas, and all the nodes operate in half-duplex mode. Since the relay is equipped with multiple antennas, the total amount of the harvested energy at the users can be significantly increased. This antenna configuration has been investigated in [25]–[27], and can be applied to scenarios in which low complexity devices communicate with each other via the help of an advanced multiple antennas node (e.g, relay). This system model is introduced as a general model which can be applied to a communication scenario in which the users are able to process information and harvest energy [28]. Hybrid protocol is adopted at the relay. Specifically, if the relay successfully decodes the users' signals, DF protocol will be adopted to forward the signals to the users, otherwise, AF protocol will be used. The $1 \times N_r$ channel vector between the source and relay is denoted by $\mathbf{h}_{sr}$, the channels between the source and the users are h_{su1},h_{su2} and the $1 \times N_r$ channel vectors between the relay and the users are denoted by $\mathbf{h}_{ru_1}$and $\mathbf{h}_{ru_2}$, respectively; all channels are modeled as quasi-static block fading channels, following a Rayleigh distribution. The distances between the source and relay is denoted by d_{sr}, the source and U1 by d_{su_1}, the source and U2 by d_{su_2}, the relay and U1 by $d_{ru_1}$and the relay and U2 by d_{ru_2}as shown in Fig. 1.

The communication between the source and users is achieved over two phases, phase I and phase II. Following the principle of NOMA, in phase I, the source broadcasts a superimposed message of U1 and U2, which will be received by the relay and the two users, part of the received signal energy will be harvested by the users to charge their batteries using the power splitting receiver. During phase II, if the signal to interference noise ratio (SINR) at the relay is larger than a threshold value, the relay uses DF protocol, otherwise the relay implements AF protocol to forward the signal to the users; again, the users harvest part of the received signal energy to charge their batteries in phase II. Therefore, NOMA has shorter time delay (latency) than conventional cooperative OMA. This is because cooperative NOMA needs only two time slots. In contrast, cooperative OMA requires four time slots, two slots for each user's message [29]. To elaborate, during the first phase, according to NOMA technique, the source transmits $x = \sqrt{P_s}\alpha_1 x_1 + \sqrt{P_s}\alpha_2 x_2$, where x_1 and x_2 are data symbols for U1 and U2 with unit variance, P_s is the source transmission power, and α_1 and α_2 are the power allocation coefficients with, $\alpha_1^2 + \alpha_2^2 \leq 1$. In the cooperative NOMA scheme considered in this paper, the users are ordered based on their average fading gains, which in the considered scenario is the same as path loss. Generally speaking, the path loss does not vary fast in a short period compared to the small-scale fading.

Hence, the distance-based users ranking can simplify the design of power allocation and rate adaption for NOMA technique [30]. Consequently, in this work, the users are ordered based on the distances information. The application of distance-based users ranking in NOMA systems has been thoroughly discussed in [30]–[33]. Without loss of generality, U1 is assumed to be closer to the source than U2, hence, we have $\alpha_1 < \alpha_2$. The received signals at the relay, U1 and U2 are, respectively, given by

$$\mathbf{y}_r = \sqrt{\frac{P_s}{d_{sr}^m}}\mathbf{h}_{sr}^T \sum_{i=1}^{2} \alpha_i x_i + \mathbf{n}_r^T, \tag{1}$$

$$y_{u_1}^{(1)} = \sqrt{\frac{\beta_1^{(1)} P_s}{d_{su1}^m}} h_{su1} \sum_{i=1}^{2} \alpha_i x_i + n_{u1}^{(1)}, \tag{2}$$

$$y_{u_2}^{(1)} = \sqrt{\frac{\beta_2^{(1)} P_s}{d_{su2}^m}} h_{su2} \sum_{i=1}^{2} \alpha_i x_i + n_{u2}^{(1)}, \tag{3}$$

where m is the path loss exponent, $0 < \beta_1^{(1)} < 1$, $0 < \beta_2^{(1)} < 1$ are the power-splitting ratios in the first phase at U1 and U2, respectively, $\mathbf{n}_r$ is the $1 \times N_r$ additive white Gaussian noise (AWGN) vector at the relay, i.e., $\mathbf{n}_r \sim \mathcal{CN}\left(0, \sigma_r^2 \mathbf{I}_{N_r}\right)$, $n_{u1}^{(1)}$ is AWGN at U1 in the first phase with variance σ_{u1}^2, $n_{u1} \sim \mathcal{CN}\left(0, \sigma_{u1}^2\right)$ and $n_{u2}^{(1)}$ is AWGN at U2 in the first phase with variance σ_{u2}^2, $n_{u2} \sim \mathcal{CN}\left(0, \sigma_{u2}^2\right)$ and T is the transpose operation. Based on NOMA, the stronger user, U1, adopts a successive interference cancellation (SIC), in which U1 first decodes the signal of the weaker user, U2, and then subtracts this component from the received signal to detect its own message. Therefore, the received SINR at U1 to detect x_2 can be written as,

$$\gamma_{x_2 \to u1}^{(1)} = \frac{a_1 \left|h_{su1}\right|^2}{b_1 \left|h_{su1}\right|^2 + c_1}, \tag{4}$$

where $a_1 = \beta_1^{(1)} P_s \alpha_2^2$, $b_1 = \beta_1^{(1)} P_s \alpha_1^2$ and $c_1 = d_{su1}^m \sigma_{u1}^2$, the rate for U1 to detect x_2, $R_{x_2 \to u1}$, should be larger than the target data rate of U2 and $\gamma_{x_2 \to u1}^{(1)}$ should be larger than target SINR of the U2 $\gamma_{th_{u2}}$. In this paper, the CSI is assumed to be perfectly known at the relay node. To know the CSI at the relay, conventional channel estimation schemes devised for point to point communications can be employed at the relay node. The source-relay channel can be known at the relay by having the source embed a pilot signal in its transmission. The optimal training design for the relay systems has been discussed in details in [34, Sec(4.5)]. Consequently, the received SINRs at U1 and U2 to detect $x_1$and x_2, and the SINR at the relay can be written, respectively, as

$$\gamma_{u1}^{(1)} = \frac{a_2 \left|h_{su1}\right|^2}{c_2}, \gamma_{u2}^{(1)} = \frac{a_3 \left|h_{su2}\right|^2}{b_3 \left|h_{su2}\right|^2 + c_3}, \tag{5}$$

$$\gamma_r^{(1)} = \frac{P_s \left\|\mathbf{h}_{sr}^T\right\|^2}{N_r d_{sr}^m \sigma_r^2}, \tag{6}$$

where $a_2 = \beta_1^{(1)} P_s \alpha_1^2$, $c_2 = \sigma_{u1}^2 d_{su_1}^m$, $a_3 = \beta_2^{(1)} P_s \alpha_2^2$, $b_3 = \beta_2^{(1)} P_s \alpha_1^2$, $c_3 = d_{su2}^m \sigma_{u2}^2$. If the relay can decode the two signals, the relay will adopt DF protocol and forward the message in the second phase with different power allocation coefficients based on the order of the users at the relay node. The relay will detect firstly x_2 and then will remove it from its received signal based on SIC. Here we define the received SINR at the relay to detect x_1, as $\gamma_{x_1 \to r}$ and the received SINR at the relay to detect x_2, as $\gamma_{x_2 \to r}$. Therefore, to successfully decode x_1 and x_2 at the relay, their effective SINRs, i.e., $\gamma_{x_1 \to r}$, and $\gamma_{x_2 \to r}$, should be larger than their corresponding target SINRs. Hence, the relay evaluates the received signal on the basis of the SINR threshold values. In order to guarantee the successful decoding, the threshold values should satisfy, $\gamma_{th_{u1}} \triangleq 2^{2R_1} - 1$ and $\gamma_{th_{u2}} \triangleq 2^{2R_2} - 1$, where R_i is the target transmission rate for user Ui, i.e., the threshold SINR values are related to predefined communication rates[1] [37]–[41]. Otherwise, if the relay cannot decode the two signals, the relay will implement AF protocol, as shown in Fig. 2. Finally, the users combine the received signals in the two phases using MRC technique[2]. Therefore, we can introduce a variable κ which is defined by

$$\kappa = \begin{cases} 1, \text{ Relay works in DF mode} \\ 0, \text{ Relay works in AF mode} \end{cases} \tag{7}$$

which is equal to one when the two conditions are satisfied, i.e., $(\gamma_{x_2 \to r} > \gamma_{th_{u2}})$ and $(\gamma_{x_1 \to r} > \gamma_{th_{u1}})$ and zero otherwise. Now, the sum-rate of the hybrid protocol can be written as

$$R = (1 - \kappa) R^{AF} + \kappa R^{DF} \tag{8}$$

where $R^{AF}$is the sum-rate in AF mode and R^{DF} is the sum-rate in DF mode. The sum-rate in cooperative systems depends on the relay capacity. In DF protocol, the decoding at the relay node is successful if and only if the transmission rate is not greater than the capacity of the source-relay link. If the desired rate is r_{ds} and

[1]Please note that, the system performance is dependent significantly on the SINR threshold values, and these values should be chosen to maximize the system performance. The optimal values of the SINR threshold values will be investigated in future work, in order to consider it with more details. In [35] it was assumed that, the relay detects whether it successfully receives the source's transmission by using a cyclic redundancy check (CRC). On the other hand, in [36], in order to get the optimal SNR threshold value, proper error criterion was adopted.

[2]The rationale for selecting MRC is because it has lower computational and implementation complexity than other well-known techniques used in such networks. In fact, MRC offers a good balance between practical complexity and satisfactory performance [42].
The received signals in the two phases, beside enhancing the system performance, will also help to increase the harvested energy at the users.

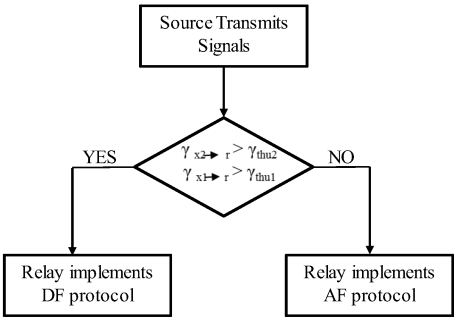

Figure 2: Hybrid relaying protocol.

the capacity of the source-relay link is C_{sr}, then outage occurs on the source-relay link if $r_{ds} > C_{sr}$. Generally speaking, the maximum achievable rate in DF mode is limited by the capacity between the source-relay, the source-destination and the relay-destination links [34]. In the AF scheme, the relay simply amplifies the received signal and forwards it directly to the destination without explicitly decoding the message [34].

III. AF Protocol

In cases when the relay is unable to decode the users' signals, the relay will work in AF mode. In the AF mode, the relay can only amplify and forward a scaled version of the received signal, i.e., in the second phase, the relay broadcasts the received signal after multiplying with an amplifying relay gain [7]. Therefore, the relay transmits signal, $\mathbf{x}_r$, given by, $\mathbf{x}_r = G\,\mathbf{y}_r$, where G is the relay gain, which assumed to be fixed and given by $G = \frac{P_r}{\mathbb{E}\left[\frac{P_s}{d_{sr}^m}\|\mathbf{h}_{sr}^T\|^2 + N_r\sigma_r^2\right]}$, where P_r is the relay transmitted power and $\mathbb{E}[.]$ is the expectation operation. The received signals at the users U1 and U2 in the second phase can be expressed, respectively, by,

$$y_{u_1}^{(2)} = \sqrt{\frac{G\beta_1^{(2)}P_s}{d_{ru1}^m d_{sr}^m}}\mathbf{h}_{ru1}\mathbf{h}_{sr}^T \sum_{i=1}^{2}\alpha_i x_i + \sqrt{\frac{G\beta_1^{(2)}}{d_{ru1}^m}}\mathbf{h}_{ru1}\mathbf{n}_r^T + n_{u1}^{(2)}, \quad (9)$$

$$y_{u_2}^{(2)} = \sqrt{\frac{G\beta_2^{(2)}P_s}{d_{ru2}^m d_{sr}^m}}\mathbf{h}_{ru2}\mathbf{h}_{sr}^T \sum_{i=1}^{2}\alpha_i x_i + \sqrt{\frac{G\beta_2^{(2)}}{d_{ru2}^m}}\mathbf{h}_{ru2}\mathbf{n}_r^T + n_{u2}^{(2)}, \quad (10)$$

where $0 < \beta_1^{(2)} < 1$, $0 < \beta_2^{(2)} < 1$ are the power-splitting ratios at U1 and U2, respectively, in the second phase, $n_{u1}^{(2)}$ is AWGN at U1 in the second phase with variance σ_{u1}^2, $n_{u1} \sim \mathcal{CN}\left(0, \sigma_{u1}^2\right)$ and $n_{u2}^{(2)}$ is AWGN at U2 in the second phase with variance σ_{u2}^2, $n_{u2} \sim \mathcal{CN}\left(0, \sigma_{u2}^2\right)$.

Again in the second phase, based on NOMA scheme the stronger user adopts SIC technique to decode its own signal. Two scenarios can be considered in the second phase.

- Firstly, the stronger user in the first phase, U1, is the stronger user in the second phase. In this case, the received SINR at U1 to detect x_2 in the second phase can be written as in (11).

The rate for U1 to detect x_2, should be larger than the target data rate of U2, i.e, $\gamma_{x_2\to u1}^{(2)}$ should be larger than target SINR of U2. Consequently, the received SINRs at U1 and U2 to detect $x_1$and x_2 in the second phase can be, respectively, written as

$$\gamma_{u1}^{(2)} = \frac{a_4\left|\mathbf{h}_{ru1}\mathbf{h}_{sr}^T\right|^2}{c_4\left\|\mathbf{h}_{ru1}\right\|^2 + d_4}, \quad (12)$$

$$\gamma_{u2}^{(2)} = \frac{a_5\left|\mathbf{h}_{ru2}\mathbf{h}_{sr}^T\right|^2}{b_5\left|\mathbf{h}_{ru2}\mathbf{h}_{sr}^T\right|^2 + c_5\left\|\mathbf{h}_{ru2}\right\|^2 + d_5}, \quad (13)$$

where $a_4 = G\beta_1^{(2)}P_s\alpha_1^2$, $c_4 = d_{sr}^m\beta_1^{(2)}G\sigma_r^2$, $d_4 = d_{sr}^m d_{ru1}^m\sigma_{u1}^2$, $a_5 = G\beta_2^{(2)}P_s\alpha_2^2$, $b_5 = G\beta_2^{(2)}P_s\alpha_1^2$, $c_5 = d_{sr}^m\beta_2^{(2)}G\sigma_r^2$, $d_5 = d_{sr}^m d_{ru2}^m\sigma_{u2}^2$. The users receive two copies of the signal in two time slots. This model is similar to single input multiple output (SIMO) systems [34].Thus, the users can perform MRC technique to maximize the received signal strength. This assumption will make the analysis complex and more challenging. Therefore, the SINR at the i^{th} user can be formulated as $\gamma_{ui} = \gamma_{ui}^{(1)} + \gamma_{ui}^{(2)}$ [17], [31], [41], [43], [44]. The sum-rate in AF mode can be written as, $R^{AF} = \sum_{i=1}^{2} R_i^{AF}$, where R_i^{AF} is the rate at user i in AF mode in bits/s/Hz and is given by,

$$R_i^{AF} = \frac{1}{2}\log_2\left(1 + \gamma_{ui}^{(1)} + \gamma_{ui}^{(2)}\right). \quad (14)$$

The average sum-rate can, hence, be expressed as

$$\mathbb{E}\left[R^{AF}\right] = \mathbb{E}\left[\sum_{i=1}^{2}\frac{1}{2}\log_2\left(1 + \gamma_{ui}^{(1)} + \gamma_{ui}^{(2)}\right)\right]. \quad (15)$$

Theorem 1. *The average sum-rate of the multiple antennas AF relaying NOMA system when one of the users (U1) is the stronger in the two phases can be obtained by*

$$\mathbb{E}\left[R^{AF}\right] = \frac{1}{2\ln(2)}\sum_{i=1}^{2}\int_0^\infty \frac{1}{z}\left(1 - \mathcal{M}_{\gamma_{ui}^{(1)}}(z)\,\mathcal{M}_{\gamma_{ui}^{(2)}}(z)\right)e^{-z}dz. \quad (16)$$

which can also be expressed in terms of the weights and abscissas of a Laguerre polynomial as

$$\mathbb{E}\left[R^{AF}\right] = \frac{1}{2\ln(2)}\sum_{i=1}^{2}\sum_{n=1}^{N}\frac{H_n}{z_n}\left(1 - \mathcal{M}_{\gamma_{ui}^{(1)}}(z_n)\,\mathcal{M}_{\gamma_{ui}^{(2)}}(z_n)\right), \quad (17)$$

$$\gamma^{(2)}_{x_2\to u_1}=\frac{G\beta_1^{(2)}P_s\alpha_2^2\left|\mathbf{h}_{ru1}\mathbf{h}_{sr}^T\right|^2}{G\beta_1^{(2)}P_s\alpha_1^2\left|\mathbf{h}_{ru1}\mathbf{h}_{sr}^T\right|^2+d_{sr}^m\beta_1^{(2)}G\left\|\mathbf{h}_{ru1}\right\|^2\sigma_r^2+d_{sr}^m d_{ru1}^m\sigma_{u1}^2}. \tag{11}$$

where $\mathcal{M}_{\gamma_{u1}^{(1)}}(z)$, $\mathcal{M}_{\gamma_{y1}^{(2)}}(z)$, $\mathcal{M}_{\gamma_{u2}^{(1)}}(z)$, $\mathcal{M}_{\gamma_{u2}^{(2)}}(z)$ are given by (18), (19), (21) and (22), respectively, and H_n, z_n are the n^{th} abscissa and weight, respectively, of the N^{th} order Laguerre polynomial, tabulated in [45, eq. (25.4.45)].

$$\mathcal{M}_{\gamma_{u1}^{(1)}}(z)=\frac{c_2}{c_2+a_2z}. \tag{18}$$

$$\mathcal{M}_{\gamma_{u1}^{(2)}}(z)=1-$$

$$z\int_0^{\infty}\frac{2\,e^{-\left(z\gamma+\frac{\gamma\,c_4}{a_4}\right)}\left(\frac{\gamma d_4}{a_4}\right)^{\frac{N_r}{2}}K_{N_r}\left(2\sqrt{d_4z}\right)}{\Gamma(N_r)}d\gamma. \tag{19}$$

$$\mathcal{M}_{\gamma_{u1}^{(2)}}(z)\approx 1-$$

$$\sum_{n=1}^{N}\mathrm{H}_n\frac{2\,e^{-\left(\gamma_n+\frac{\gamma_n\,c_4}{z\,a_4}\right)}\left(\frac{\gamma_n\,d_4}{z\,a_4}\right)^{\frac{N_r}{2}}K_{N_r}\left(2\sqrt{d_4z}\right)}{\Gamma(N_r)}. \tag{20}$$

$$\mathcal{M}_{\gamma_{u2}^{(1)}}(z)=\int_0^{\frac{a_3}{b_3}}\frac{e^{-z\gamma}\,a_3\,c_3}{(a_3-\gamma b_3)^2}\,e^{-\frac{c_3\gamma}{a_3-b_3\gamma}}\,d\gamma. \tag{21}$$

$$\mathcal{M}_{\gamma_{u2}^{(2)}}(z)=1-$$

$$z\int_0^{\frac{a_5}{b_5}}\frac{2\,e^{-\left(z\gamma+\frac{\gamma c_5}{a_5-\gamma b_5}\right)}\left(\frac{\gamma d_5}{a_5-\gamma b_5}\right)^{\frac{N_r}{2}}K_{N_r}\left(2\sqrt{d_5z}\right)}{\Gamma(N_r)}d\gamma. \tag{22}$$

Proof: The proof is provided in Appendix A. ■

- Secondly, the stronger user in the first phase, U1, is the weaker user in the second phase. Generally speaking, in this scenario U1 might not be able to detect the messages in the second phase, and this scenario might lead to outage at U1 in the second phase. However, U1 can decode it is own message based on its reception in the first phase, exploiting the diversity provided in relaying systems, i.e., if one link to the user is failed, the signal can still be received by the user through the other link. The average sum-rate of this scenario can be easily obtained by substituting $\mathcal{M}_{\gamma_{u1}^{(2)}}(z)=1$ in the derived expression in (16) provided in Theorem 1.

IV. DF Protocol

In the case when the relay can successfully decode $x_1$and x_2, the relay can adopt DF protocol. The relay detects x_2 firstly by treating x_1 as a noise and then will remove it from its received signal based on SIC. The capacity enhancement that can be achieved by DF protocol might come on the expense of latency, since the decoding process incur additional time delay. However, this delay is much shorter than a time slot and its impact on the total achievable rate can be negligible [46]. Therefore, the received SINR at the relay for decoding x_2 and $x_1$are given by,

$$\gamma_{x_2\to r}=\frac{a_6\left\|\mathbf{h}_{sr}^T\right\|^2}{b_6\left\|\mathbf{h}_{sr}^T\right\|^2+c_6},\ \text{and}\ \gamma_{x_1\to r}=a_7\left\|\mathbf{h}_{sr}^T\right\|^2, \tag{23}$$

where $a_6=P_s\alpha_2^2$, $b_6=P_s\alpha_1^2$, $c_6=N_rd_{sr}^m\sigma_r^2$, $a_7=\frac{P_s\alpha_1^2}{N_rd_{sr}^m\sigma_r^2}$, with satisfying the conditions $\gamma_{x_2\to r}>\gamma_{th_{u2}}$ and $\gamma_{x_1\to r}>\gamma_{th_{u1}}$. Then, the relay transmits a superimposed composite signal, $\mathbf{x}_r=\sqrt{P_r}\sum_{i=1}^{2}\mathbf{w}_i\rho_i\,x_i$, where ρ_1, ρ_2 are the power allocation coefficients in the second phase with, $\rho_1^2+\rho_2^2\le 1$, and $\mathbf{w}_i$ is $1\times N_r$ precoding vector. Consequently, the received signals at the users in the second phase are, respectively,

$$y_{u_1}^{(2)}=\sqrt{\frac{\beta_1^{(2)}P_r}{d_{ru1}^m}}\mathbf{h}_{ru1}\sum_{i=1}^{2}\mathbf{w}_i^T\rho_ix_i+n_{u1}^{(2)}. \tag{24}$$

$$y_{u_2}^{(2)}=\sqrt{\frac{\beta_2^{(2)}P_r}{d_{ru2}^m}}\mathbf{h}_{ru2}\sum_{i=1}^{2}\mathbf{w}_i^T\rho_ix_i+n_{u2}^{(2)}. \tag{25}$$

In the second phase, based on NOMA, the stronger user adopts SIC technique. In this scenario the stronger user in the first phase might be the weaker or stronger in the second phase, which makes the analysis of this scenario more complicated. Hence, we can find the possible cases shown in Table I.

	Phase I		Phase II	
Case I	U1 strong	U2 weak	U1 strong	U2 weak
Case II	U1 strong	U2 weak	U1 weak	U2 strong

Table I: Possible cases of the users in the two phases.

Assuming the i^{th} user is the stronger user. Hence based on the transmit diversity scheme, the received SINR at the stronger user, Ui, to detect the signal of the weaker user $(x_{\bar{i}})$ in the second phase can be formulated as,

$$R_1^{DF} = \frac{1}{2}\min\left[\log_2\left(1+\gamma_{x_1\to r}\right), \log_2\left(1+\gamma_{u1}^{(1)}+\gamma_{u1}^{(2)}\right)\right], \tag{28}$$

$$R_2^{DF} = \frac{1}{2}\min\left[\log_2\left(1+\gamma_{x_2\to u1}^{(1)}\right), \log_2\left(1+\gamma_{x_2\to r}\right), \log_2\left(1+\gamma_{x_2\to u1}^{(2)}\right), \log_2\left(1+\gamma_{u2}^{(1)}+\gamma_{u2}^{(2)}\right)\right] \tag{29}$$

$$\gamma_{x_{\bar{i}}\to ui}^{(2)} = \frac{a_8\left\|\mathbf{h}_{rui}\right\|^2}{b_8\left\|\mathbf{h}_{rui}\right\|^2 + c_8}, \tag{26}$$

where $a_8 = \beta_i^{(2)} P_r \rho_{\bar{i}}^2$, $b_8 = \psi_{\bar{i}}\beta_i^{(2)} P_r \rho_i^2$, $c_8 = d_{sui}^m \sigma_{ui}^2$, while $i, \bar{i} \in \{1,2\}$, $i \neq \bar{i}$ and

$$\psi_1 = \begin{cases} 1 & \text{If U2 is stronger in PhaseII} \\ 0 & \text{If U1 is stronger in PhaseII} \end{cases}$$

and $\psi_2 = 1-\psi_1$, with satisfying the condition, $\gamma_{x_{\bar{i}}\to ui} > \gamma_{th_{u\bar{i}}}$. Consequently, based on the transmit diversity scheme, the received SINRs at U1 and U2 to detect x_1 and x_2 in the second phase can be written, as

$$\gamma_{ui}^{(2)} = \frac{\beta_i^{(2)} P_r \rho_i^2 \left\|\mathbf{h}_{rui}\right\|^2}{\psi_i \beta_i^{(2)} P_r \rho_{\bar{i}}^2 \left\|\mathbf{h}_{rui}\right\|^2 + d_{rui}^m \sigma_{ui}^2}. \tag{27}$$

where $i, \bar{i} \in \{1,2\}$, $i \neq \bar{i}$. The users perform MRC technique, and the total SINRs at the i^{th} user is,$\gamma_{ui} = \gamma_{ui}^{(1)} + \gamma_{ui}^{(2)}$. The total sum-rate in DF mode, $R^{DF} = \sum_{i=1}^{2} R_i^{DF}$, can be calculated based on the users order in the second phase, as it is explained in the next two cases.

- Case 1 $\psi_1 = 0$:

In this case U1 is also the stronger user in the second phase and U2 is weaker in the two phases, in this scenario the rates at U1 and U2 can be given by[3] (28) and (29) [6].

Therefore, the average rates can be calculated by averaging the instantaneous rate expressions in (28) and (29).

Theorem 2. *The average sum-rate of the multiple antennas DF relaying NOMA system when one of the users (U1) is the stronger in the two phases can be obtained by (30) and (31), where $\mathcal{M}_{\gamma_{u1}^{(1)}}(z)$, $\mathcal{M}_{\gamma_{u2}^{(1)}}(z)$ have been derived in (18) & (21), respectively, and* $\mathcal{M}_{\gamma_{u1}^{(2)}}(z) = \left(1+\frac{a_9}{c_9}z\right)^{-N_r}$, $\mathcal{M}_{\gamma_{u2}^{(2)}}(z) = \frac{1}{\Gamma(N_r)}\int_0^{\frac{a_{10}}{b_{10}}} e^{-\gamma\left(z+\frac{c_{10}}{a_{10}-b_{10}\gamma}\right)}\left(\frac{c_{10}\gamma}{a_{10}-b_{10}\gamma}\right)^{N_r-1} \times\left(\frac{b_{10}c_{10}\gamma}{(a_{10}-b_{10}\gamma)^2}+\frac{c_{10}}{a_{10}-b_{10}\gamma}\right)d\gamma$, $a_9 = \beta_1^{(2)}P_r\rho_1^2$, $b_9 = \psi_1\beta_1^{(2)}P_r\rho_2^2$, $c_9 = d_{ru1}^m\sigma_{u1}^2$, $a_{10} = \beta_2^{(2)}P_r\rho_2^2$, $b_{10} = \psi_2\beta_2^{(2)}P_r\rho_1^2$ *and* $c_{10} = d_{ru2}^m\sigma_{u2}^2$.

Proof: The proof is provided in Appendix B. ■

- Case 2 $\psi_1 = 1$:

In this case, U1 is the weaker user in the second phase and U2 is the stronger in the second phase. In this scenario, the rates at U1 and U2 can be given by (32) and (33) [6], [34].

Therefore, the average rates can be calculated by averaging the instantaneous rate expressions in (32) and (33).

Theorem 3. *The average sum-rate of the multiple antennas DF relaying NOMA system when one user (U1) is stronger in first phase and the other user (U2) is stronger in second phase can be obtained by (34) and (35), where $\mathcal{M}_{\gamma_{u1}^{(1)}}(z)$, $\mathcal{M}_{\gamma_{u2}^{(1)}}(z)$ have been derived in (18) & (21), respectively, and* $\mathcal{M}_{\gamma_{u1}^{(2)}}(z) = \frac{1}{\Gamma(N_r)}\int_0^{\frac{a_9}{b_9}} e^{-\gamma\left(z+\frac{c_9}{a_9-b_9\gamma}\right)}\left(\frac{c_9\gamma}{a_9-b_9\gamma}\right)^{N_r-1} \times\left(\frac{b_9c_9\gamma}{(a_9-b_9\gamma)^2}+\frac{c_9}{a_9-b_9\gamma}\right)d\gamma$, $\mathcal{M}_{\gamma_{u2}^{(2)}}(z) = \left(1+\frac{a_{10}}{c_{10}}z\right)^{-N_r}$.

Proof: The proof is provided in Appendix B. ■

V. Untrusted Relay

In this section, we consider the case when the relay is an untrusted node, and may act as both helper and eavesdropper at the same time. The transmitted messages must hence remain secret when using the relay for forwarding the signal. Therefore, cooperative jamming technique with three time slots is considered to degrade the received SINR at the relay node and to enforce the relay to work always in the AF mode. In the first phase, time slot $\tau\,\mathsf{T}$, where $0<\tau<1$ and T is a block transmission time, the source and the relay transmit energy signals to charge the users. In the second phase, time slot $(1-\tau)\,\mathsf{T}/2$, while the source transmits the message, the two users cooperate to transmit the jamming signal. For simplicity, the strong user U1 is chosen to transmit a jamming signal (v) to degrade the SINR at the relay node using the harvested energy, and the weak user can save his energy for future use [4]. In the third phase, time slot $(1-\tau)\,\mathsf{T}/2$, the relay amplifies and forwards the received signal to the users. In this scenario, we assume that the channel between the two users is strong, which can be guaranteed in

[3]Please note that, in DF scheme if the relay is able to decode the source message, the relay will regenerate the same message and forward it to the destination in the second phase. Thus, the destination will receive two copies of the signal in two phases, and MRC can be applied to maximize the SINR [34, (3.22)].

[4]Please note that, the system security can be enhanced by enforcing the weak user, as well as the strong user, to transmit a jamming signal in the second phase.

$$\mathbb{E}\left[R_1^{DF}\right] = \frac{1}{2}\min\left[\int_0^\infty \frac{e^{-z}}{z\ln 2}\left(1-(1+a_7 z)^{-N_r}\right)dz,\ \int_0^\infty \frac{e^{-z}}{z\ln 2}\left(1-\mathcal{M}_{\gamma_{u1}^{(1)}}(z)\,\mathcal{M}_{\gamma_{u1}^{(2)}}(z)\right)dz\right]. \quad (30)$$

$$\mathbb{E}\left[R_2^{DF}\right] = \frac{1}{2}\min\Bigg[\int_0^\infty \frac{e^{-zc_1}}{z\ln 2}\left(\frac{1}{1+b_1 z}-\frac{1}{1+(a_1+b_1)z}\right)dz,$$

$$\int_0^\infty \frac{e^{-zc_6}}{z\ln 2}\left((1+b_6 z)^{-N_r}-(1+(a_6+b_6)z)^{-N_r}\right)dz,$$

$$\int_0^\infty \frac{e^{-zc_8}}{z\ln 2}\left((1+b_8 z)^{-N_r}-(1+(a_8+b_8)z)^{-N_r}\right)dz,\ \int_0^\infty \frac{e^{-z}}{z\ln 2}\left(1-\mathcal{M}_{\gamma_{u2}^{(1)}}(z)\,\mathcal{M}_{\gamma_{u2}^{(2)}}(z)\right)dz\Bigg] \quad (31)$$

$$R_1^{DF} = \frac{1}{2}\min\left[\log_2(1+\gamma_{x_1\to r}),\ \log_2\left(1+\gamma_{u1}^{(1)}+\gamma_{u1}^{(2)}\right),\log_2\left(1+\gamma_{x_1\to u2}^{(2)}\right)\right], \quad (32)$$

$$R_2^{DF} = \frac{1}{2}\min\left[\log_2\left(1+\gamma_{x_2\to u_1}^{(1)}\right),\log_2(1+\gamma_{x_2\to r}),\ \log_2\left(1+\gamma_{u2}^{(1)}+\gamma_{u2}^{(2)}\right)\right], \quad (33)$$

$$\mathbb{E}\left[R_1^{DF}\right] = \frac{1}{2}\min\Bigg[\int_0^\infty \frac{e^{-z}}{z\ln 2}\left(1-(1+a_7 z)^{-N_r}\right)dz,\ \frac{1}{\ln(2)}\int_0^\infty \frac{e^{-z}}{z}\left(1-\mathcal{M}_{\gamma_{u1}^{(1)}}(z)\,\mathcal{M}_{\gamma_{u1}^{(2)}}(z)\right)dz,$$

$$\int_0^\infty \frac{1}{z\ln 2}\left((1+b_8 z)^{-N_r}-(1+(a_8+b_8)z)^{-N_r}\right)e^{-zc_8}dz\Bigg], \quad (34)$$

$$\mathbb{E}\left[R_2^{DF}\right] = \frac{1}{2}\min\Bigg[\int_0^\infty \frac{e^{-zc_1}}{z\ln 2}\left(\frac{1}{1+b_1 z}-\frac{1}{1+(a_1+b_1)z}\right)dz,$$

$$\int_0^\infty \frac{e^{-zc_6}}{z\ln 2}\left((1+b_6 z)^{-N_r}-(1+(a_6+b_6)z)^{-N_r}\right)dz,\ \int_0^\infty \frac{e^{-z}}{z\ln 2}\left(1-\mathcal{M}_{\gamma_{u2}^{(1)}}(z)\,\mathcal{M}_{\gamma_{u2}^{(2)}}(z)\right)dz\Bigg], \quad (35)$$

NOMA systems by paring the two users who are close. Consequently, the jamming can be designed to degrade the SINR at the relay and demodulated by the weak user[5], as studied in [47]. Since all the nodes in the system model operate in half-duplex mode, the two users can receive their information signals only in the third time slot through the relay node. Consequently, the received signal at the relay in the second time slot is expressed by

$$\mathbf{y}_r = \sqrt{\frac{P_s}{d_{sr}^m}}\mathbf{h}_{sr}^T\sum_{i=1}^{2}\alpha_i x_i + \sqrt{\frac{P_{u1}}{d_{ru1}^m}}\mathbf{h}_{u1r}^T v + \mathbf{n}_r^T, \quad (36)$$

where $\mathbf{h}_{u1r}$ is the $1\times N_r$ channel vector between U1 and the relay, and P_{u1} is the harvested power at U1 during power transfer phase and is given by

$$P_{u1} = \frac{2\eta_1\tau}{(1-\tau)}\left[\frac{P_s}{d_{su1}^m}\left|\overline{h_{su1}}\right|^2 + \frac{P_r}{d_{ru1}^m}\left\|\overline{\mathbf{h}_{ru1}}\right\|^2\right], \quad (37)$$

where $\overline{h_{su1}}$, and $\overline{\mathbf{h}_{ru1}}$ denote the channels in the power transmission phase. As we have mentioned, if the relay can detect x_2, it will use SIC to detect x_1, therefore, our concern will be on the secrecy of the U2 (weak user). The SINR at the relay to detect the weak user's signal is

$$\gamma_{x_2\to r} = \frac{P_s\alpha_2^2 d_{ru1}^m\left\|\mathbf{h}_{sr}^T\right\|^2}{P_s\alpha_1^2 d_{ru1}^m\left\|\mathbf{h}_{sr}^T\right\|^2 + P_{u1}d_{sr}^m\left\|\mathbf{h}_{u1r}^T\right\|^2 + N_r\sigma_r^2 d_{sr}^m d_{ru1}^m}, \quad (38)$$

Substituting (37) in (38), the SINR at the relay becomes as in (39), where $\varrho_{11} = P_s\alpha_2^2 d_{u1r}^m$, $a_{11} =$

[5]Please note that, if the source transmission in the second phase is too strong, the SINR at the relay will be high, and too much jamming power is needed to degrade it.

$$\gamma_{x_2\to r}=\frac{\varrho_{11}\left\|\mathbf{h}_{sr}^{T}\right\|^{2}}{a_{11}\left\|\mathbf{h}_{sr}^{T}\right\|^{2}+b_{11}\left\|\mathbf{h}_{u1r}^{T}\right\|^{2}\left|\overline{h_{su1}}\right|^{2}+c_{11}\left\|\mathbf{h}_{u1r}^{T}\right\|^{2}\left\|\overline{\mathbf{h}_{ru1}}\right\|^{2}+r_{11}}, \tag{39}$$

$P_s\alpha_1^2 d_{u1r}^m$, $b_{11}=\frac{2d_{sr}^m\eta_1\tau P_s}{d_{su1}^m(1-\tau)}$, $c_{11}=\frac{2d_{sr}^m\eta_1\tau P_r}{d_{ru1}^m(1-\tau)}$, $r_{11}=N_r\sigma_r^2 d_{sr}^m d_{u1r}^m$. The rate at the relay is given by, $R_{ru2}=\frac{(1-\tau)}{2}\log\left(1+\gamma_{x_2\to r}\right)$. The SINR at the relay to decode x_2 depends on the system channels in the power and information phases, which will make the analysis of this scenario more interesting. On the other hand, since the two users know the jamming signal, the users can subtract the jamming signal component v from their received signals in the third phase. Therefore, the received signals in the third phase at U1 and U2 can be expressed as in (9) and (10), respectively, with the relay gain now given by, $G=\frac{P_r}{\mathbb{E}\left[\frac{P_s}{d_{sr}^m}\|\mathbf{h}_{sr}^T\|^2+\frac{P_{u1}}{d_{ru1}^m}\left\|\mathbf{h}_{u1r}^T\right\|^2+N_r\sigma_r^2\right]}$.

Theorem 4. *The average secrecy rate in cooperative NOMA with an untrusted relay is given by [48, page 4692] [49, Eq(5)]*

$$R_s=\left[\mathbb{E}\left(R_{u2}\right)-\mathbb{E}\left(R_{ru2}\right)\right]^{+}, \tag{40}$$

where the average rate at U2 $\mathbb{E}\left(R_{u2}\right)$ and at the relay $\mathbb{E}\left(R_{ru2}\right)$ are given by (41) and (42), respectively.

$$\mathbb{E}\left(R_{u2}\right)=\frac{(1-\tau)}{2\ln 2}\int_0^\infty\frac{1}{z}\left(\left(\frac{1}{1+b_5 z}\right)-\left(\frac{1}{1+\left(a_5+b_5\right)z}\right)\right)\times\left(\frac{2\left(d_5 z\right)^{\frac{N_r}{2}}}{\Gamma\left(N_r\right)}\mathrm{J}\left(N_r,2\sqrt{d_5 z}\right)\right)e^{-zc_5}dz, \tag{41}$$

$$\mathbb{E}\left(R_{ru2}\right)=\frac{(1-\tau)}{2\ln 2}\int_0^\infty\frac{1}{z}\left(\mathcal{M}_K\left(z\right)-\mathcal{M}_W\left(z\right)\right)\times\mathcal{M}_L\left(z\right)\mathcal{M}_\Theta\left(z\right)dz, \tag{42}$$

while,

$$\mathcal{M}_K\left(z\right)=\int_0^\infty\frac{e^{-r_{11}zx}}{\Gamma\left(N_r\right)}\left(1+a_{11}xz\right)^{-N_r}x^{(-N_r-1)}e^{-\frac{1}{x}}dx, \tag{43}$$

$$\mathcal{M}_K\left(z\right)=\sum_{n=1}^{N}\frac{\mathrm{H}_n}{r_{11}z\Gamma\left(N_r\right)}\left(1+\frac{a_{11}x_n z}{r_{11}z}\right)^{-N_r}\times\left(\frac{x_n}{r_{11}z}\right)^{(-N_r-1)}e^{-\frac{r_{11}z}{x_n}}, \tag{44}$$

$$\mathcal{M}_W\left(z\right)=\int_0^\infty\frac{e^{-r_{11}zx}}{\Gamma\left(N_r\right)}\left(1+\left(a_{11}+\varrho_{11}\right)xz\right)^{-N_r}x^{(-N_r-1)}e^{-\frac{1}{x}}dx, \tag{45}$$

$$\mathcal{M}_W\left(z\right)=\sum_{n=1}^{N}\frac{\mathrm{H}_n}{r_{11}z\Gamma\left(N_r\right)}\left(1+\frac{\left(a_{11}+\varrho_{11}\right)x_n z}{r_{11}z}\right)^{-N_r}\times\left(\frac{x_n}{r_{11}z}\right)^{(-N_r-1)}e^{-\frac{r_{11}z}{x_n}}, \tag{46}$$

$$\mathcal{M}_L\left(z\right)=\frac{1}{1+b_{11}z},\qquad\mathcal{M}_\Theta\left(z\right)=\left(1+c_{11}z\right)^{-N_r}. \tag{47}$$

Proof: The proof is provided in Appendix C. ■

VI. Numerical Results

In this section, we present numerical results of the analytical expressions derived in this work. Monte Carlo simulations with 10^6 independent trials are conducted, in each simulation run channel coefficients are randomly generated. Unless stated otherwise, $P_s=P_r=P$, the noise power at all nodes are set as $\sigma_r^2=\sigma_{u1}^2=\sigma_{u2}^2=\sigma^2=0$ dBw, the path loss exponent $m=2.7$, $\eta=0.8$ [50], the power allocation coefficients α_i^2, $\rho_i^2=\frac{2-i+1}{\mu}$, with μ is chosen to satisfy $\sum_{i=1}^{2}\alpha_i^2=1$, $\sum_{i=1}^{2}\rho_i^2=1$. For illustration purposes, we consider a simple one-dimensional model, where all nodes are located on a straight line, and the source and the users, are placed at (0, 0) m, (d_{su1}, 0) m and (d_{su2}, 0) m, respectively. In addition, for simplicity, but without loss of generality, we consider fixed power-splitting ratios scheme, i.e., setting fixed power-splitting ratios $\beta_1^{(1)}=\beta_2^{(1)}=\beta_1^{(2)}=\beta_2^{(2)}=0.95$ [51], [52].

A. AF Protocol

Here we investigate the impact of SNR, number of the relay antennas and the relay position on the system performance in AF relaying mode. The analytical results for this section are obtained from Theorem 1.

In order to demonstrate the impact of SNR=$\frac{P}{\sigma^2}$, on the system performance in AF relaying case, we plot Fig. 3, which includes the rates of U1, U2 and the sum-rate versus SNR for various values of N_r when $d_{sr}=2.5m$, $d_{su1}=2m$, and $d_{su2}=5m$. For the sake of comparison, results for the OMA scheme (conventional transmission) are also included in Fig. 3. It is evident from these results, as expected, that the rates

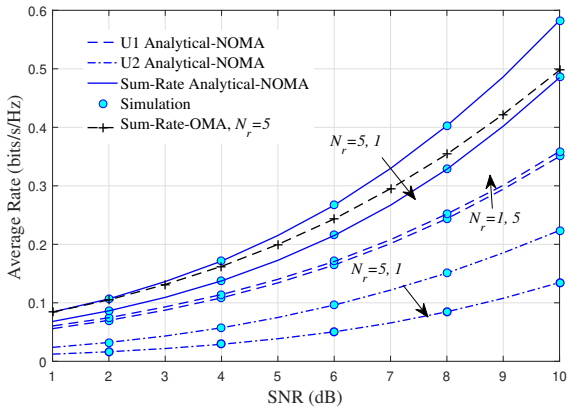

Figure 3: Average rates versus SNR for various values of N_r, when the relay is in AF mode.

improve with increasing SNR. The other observation is that, the system performance enhances as N_r is increased, however, this enhancement is more obvious at the farther user U2. This can be intuitively explained as follows, the SINR at U2 in the first phase is low and the performance of this user depends essentially on the relay transmission in the second phase. On the contrary, U1 has strong SINR from the direct link. Comparing the performance of NOMA technique with OMA, one can observe that, NOMA outperforms OMA for the considered system feature, and the gap performance between NOMA and conventional OMA becomes wider as the SNR increases.

Fig. 4 depicts a plot for the system rates as a function of d_{sr}. System parameters adopted in this figure are $N_r = 5$, $d_{su1} = 3m$, and $d_{su2} = 6m$ and SNR= 10dBW. The figure shows that the system rates are at their minimum when the relay is far away from the source. The figure also reveals that, the performance of U1 (stronger user) is sensitive to the position of the relay node, whereas the weaker user performance (U2) remains almost steady for when $1m < d_{sr} < 5m$. This happens because, d_{sr} has similar impact on both the information signal of U2 and the interference at U2 (U1 signal), and as a result, the benefit of this location changing might not affect the weaker user significantly. On contrary, at the stronger user U1, changing d_{sr} will impact on the information signal power and thus on the U1 performance. In the setting considered here, the best relay position for U1 is at $1.5m$.

B. DF Protocol

Similarly here we investigate the impact of SNR, number of the relay antennas and the relay position on the system performance in DF mode, for same system features in AF relaying mode. The analytical results for this section are obtained from Theorem 2 and Theorem 3.

Fig. 5 shows the system rates versus the SNR for different values of the relay antennas N_r when U1 is the stronger user in the two phases as in Fig. 5a and when U1 is the stronger user in the first phase and U2 is the stronger user in the second phase, as in Fig. 5b. For the sake of comparison, results for the OMA scheme are also included in Fig. 5a and Fig. 5b. From the two figures, we observe that, as in AF relaying mode, the rate at the users enhance with increasing the SNR and number of the relay antennas. Interestingly enough, however, it is clear that U2 has better performance, larger data rate, than U1 at low SNR, while, at higher SNRs, the data rate of U1 becomes greater than that of U2. Comparing the two cases, one can observe that, in the first case U1 trend to have better data rate at around SNR=16.7 dBW for $N_r = 1$ and SNR=17.1 dBW for $N_r = 5$. However, in the second case when U2 is the stronger in the second phase, U1 outperforms U2 at higher SNR which is around SNR=23.5 dBW for $N_r = 1$ and SNR=24 dBW for $N_r = 5$. Finally, it is evident that in the two scenarios, NOMA has better performance than OMA for the same system parameters.

To illustrate the impact of the distance between the relay and the source on the system performance, we plot in Fig. 6 the rates versus d_{sr}, when $N_r = 5$, $d_{su1} = 3m$, and $d_{su2} = 6m$ and SNR= 10dBW. In this figure, when the relay is near a user this user will be the stronger one in the second phase. Having a closer look at this figure, two main observations can be noticed. Firstly, the system performance degrades as the relay moves away from the source and that there exists an optimal position for the relay for each user that maximizes the data rate. Secondly, when the relay is close to the source, in the sense that U1 is the stronger in the second phase as well, U1 has higher data rate than the second user U2. However, the data rate of U1 degrades as the relay moves towards U2, and when $d_{sr} > 2.5m$ the data rate at U2 becomes larger than that of U1, and this trend confirms our results in the previous figure.

In order to provide more explanation of how the hybrid protocol performance can be compared with only AF or DF protocols, Fig. 7 shows the average sum-rates of hybrid, only DF and only AF protocols when the target data rate is 0.35, 0.75, 1 and 1.25 bits/s/Hz,

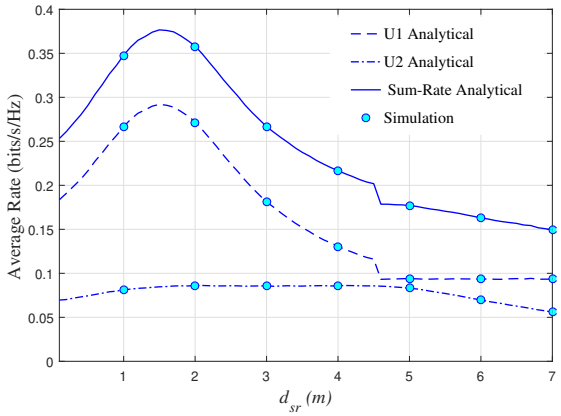

Figure 4: Average rates versus d_{sr}, when the relay is in AF mode.

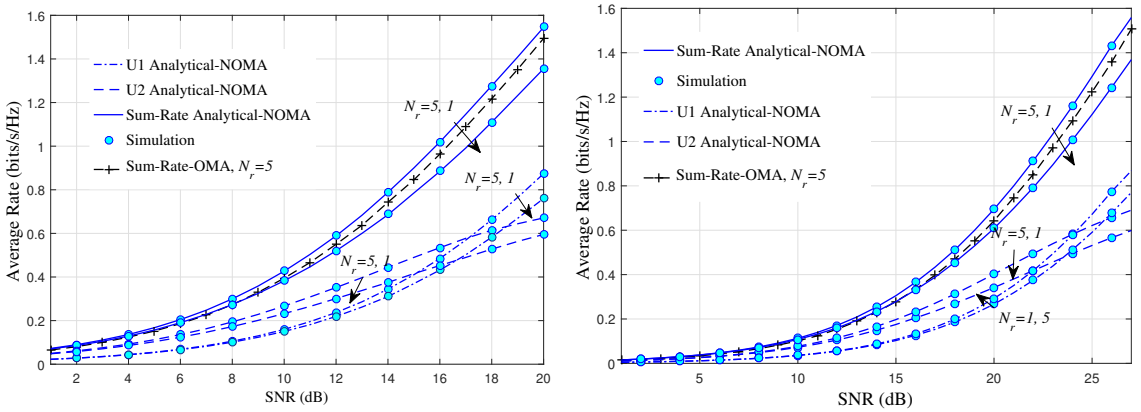

(a) Average rates versus SNR for various values of N_r, when U1 is the strong in the two phases, $d_{sr} = 2.5m$, $d_{su1} = 2m$, and $d_{su2} = 5m$.

(b) Average rates versus SNR for various values of N_r, when U2 is the strong in the second phase, $d_{sr} = 4.5m$, $d_{su1} = 2m$, and $d_{su2} = 5m$.

Figure 5: Average rates versus SNR for various values of N_r when the relay is in DF mode.

respectively. From this figure, it is clear that the system performance depends significantly on the value of the target rate, and this value should be chosen carefully to maximize the system performance. The figure shows that, when the target rate is 0.35 bits/s/Hz, the hybrid protocol can take the advantages of both AF and DF protocols, therefore, it works as DF when DF is the best and as AF when AF has better performance.

C. UN-Trusted Relay

We now investigate the effect of the EH time duration τ, the SNR value, number of relay antennas and the relay location on the maximum achievable secrecy rate of the proposed system.

Fig. 8 shows the numerical and simulation results of the U2 secrecy rate versus the EH time duration τ for different values of the SNR, with $d_{sr} = 2.5m$, $d_{su1} = 2m$, $d_{su2} = 3m$ and $N_r = 30$. Notably, and as anticipated, for each SNR value there is optimal value of the EH time duration τ that maximize the secrecy rate. This can be explained by the fact that, when τ is short the stronger user cannot harvest enough energy to jam the relay in the second phase. On contrast, when τ is too long, short time duration will be allocated for the information transmission in phases II and III. Final notice from this result is that, the secrecy rate enhances as the SNR increases.

To illustrate the impact of d_{sr} and N_r on the secrecy rate, we plot in Fig. 9 the average secrecy rate versus d_{sr} for several values of N_r when $d_{su1} = 0.5m$ and $d_{su2} = 3m$ and SNR $= 10$ dBw. The first observation here is that, as number of the relay antennas N_r increases the average secrecy rate enhances and this enhancement becomes less significant when N_r is relatively high. The other interesting observation from this figure is that for each value of N_r, there is an optimal value of d_{sr} that optimizes the secrecy rate. This is because when the relay is closed to the source and U1, the received information signal at the relay in the second phase will be stronger than the jamming signal due to the fact that the source power is higher than the harvesting power at U1. However, as the relay moves away from the source the strength of the received information signal reduces while the strength of the jamming signal increases until the secrecy rate reaches its maximum point. For long

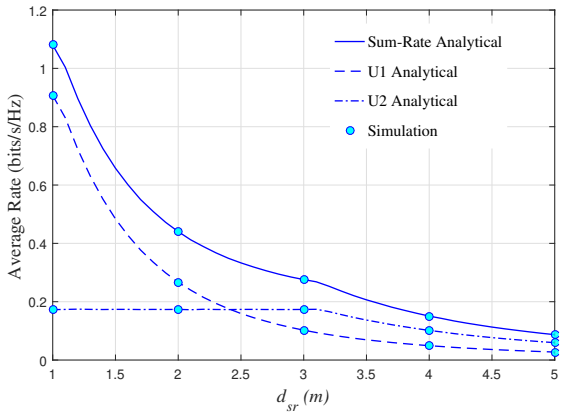

Figure 6: Average rates versus d_{sr}, when the relay is in DF mode.

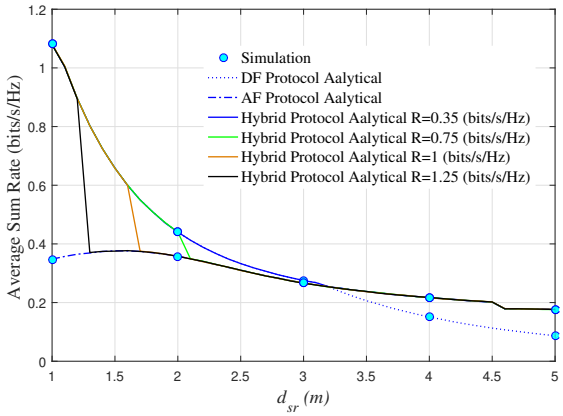

Figure 7: Average sum-rates versus d_{sr}, when the relay is in hybrid, only DF, and only AF modes, for different values of the target data rate.

distances, the harvested power at U1 will not be strong enough to protect the information signal due to the impact of the larger path loss.

VII. Conclusion

In this paper, we investigated the performance of NOMA in cooperative systems when a source node communicates with two EH user equipments via a multiple antennas hybrid AF/DF relaying node. Firstly, we derived new accurate analytical expressions for the average sum-rates in AF and DF relaying modes. Secondly, we extended the investigation to the scenario when the relay is an untrusted node, and new accurate analytical expressions for the average secrecy rate was derived. The results demonstrated that the relay position is the key to achieve best performance and the proper selection of the EH time duration is the key to maximize the secrecy rate. Also, increasing the SNR value and the number of antennas at the relay node can considerably enhance the performance of the proposed systems.

Appendix A

In this appendix we derive the average sum-rate expression presented in Theorem 1. By using the identities in [53], for all $x > 0$ we can write

$$\ln\left(1+\left(x_1+x_2\right)\right) = \int_0^{\infty} \frac{1}{z}\left(1-e^{-z\left(x_1+x_2\right)}\right) e^{-z}\,\mathrm{d}z. \tag{48}$$

Assuming $x_1$and x_2 independent random variables, and then the average of (48) can be found as

$$\mathbb{E}\left[\ln\left(1+\left(x_1+x_2\right)\right)\right] = \int_0^{\infty} \frac{1}{z}\left(1-\mathcal{M}_{x_1}\left(z\right)\mathcal{M}_{x_2}\left(z\right)\right) e^{-z}\,\mathrm{d}z, \tag{49}$$

where $\mathcal{M}_{x_1}\left(z\right)$ is the the moment generating function (MGF) of x_1 and $\mathcal{M}_{x_2}\left(z\right)$ is the MGF of x_2. Therefore, the average rate at a user i can be expressed as

$$\mathbb{E}\left[R_i\right] = \frac{1}{2\ln\left(2\right)}\int_0^{\infty} \frac{1}{z}\left(1-\mathcal{M}_{\gamma_{ui}^{(1)}}\left(z\right)\mathcal{M}_{\gamma_{ui}^{(2)}}\left(z\right)\right) e^{-z} dz, \tag{50}$$

where $\mathcal{M}_{\gamma_{ui}^{(1)}}\left(z\right)$ is the MGF of $\gamma_{ui}^{(1)}$ and $\mathcal{M}_{\gamma_{ui}^{(2)}}\left(z\right)$ is the MGF of $\gamma_{ui}^{(2)}$. The MGF of any random variable γ is defined as$\mathcal{M}_{\gamma}\left(z\right) = \int_{-\infty}^{\infty} e^{-z\gamma} f\left(\gamma\right) d\gamma$, where $f\left(\gamma\right)$ is the probability density function (PDF) of γ. Now using the fact that, $\gamma_{u1}^{(1)}$ follows Exponential distribution, the MGF of $\gamma_{u1}^{(1)}$ can be found as in (18). However, in this

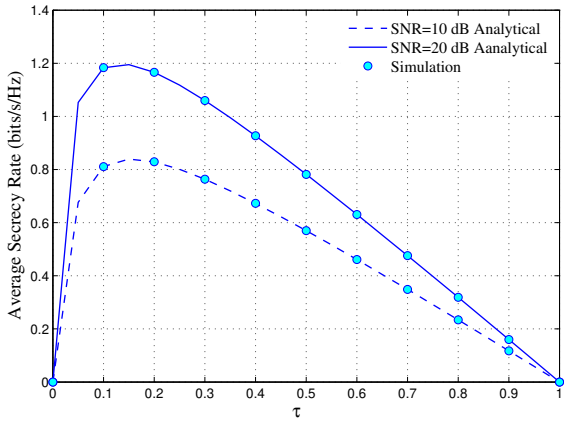

Figure 8: Rate and the secrecy rate as a function of τ for different values of the SNR.

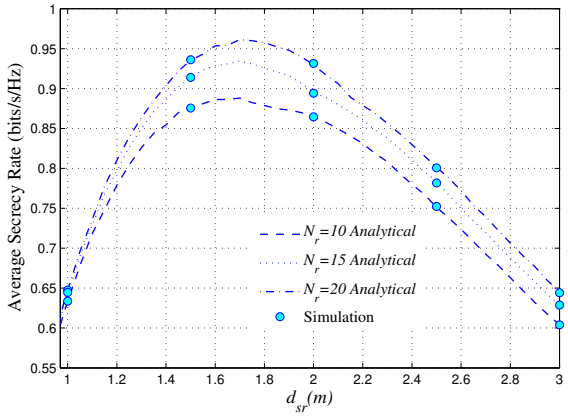

Figure 9: Average secrecy rate as a function of d_{sr} for different values of N_r.

appendix will provide the MGF of a general form of $\gamma_{ui}^{(1)}$which is given by $\gamma_{ui}^{(1)} = \frac{a_j|h_{sui}|^2}{b_j|h_{sui}|^2+c_j}$, where $j=2$ for U1 and $j=3$ for U2, and $b_2=0$. To find the PDF of $\gamma_{ui}^{(1)}$, let's start with deriving the cumulative distribution function (CDF) of $\gamma_{ui}^{(1)}$, as follow

$$F_{\gamma_{ui}^{(1)}}(\gamma) = \Pr\left(\frac{a_j|h_{sui}|^2}{b_j|h_{sui}|^2+c_j} < \gamma\right), \quad (51)$$

where $\Pr(a<b)$ shows the probability of a being less than b. (51) can now be further simplified as $F_{\gamma_{ui}^{(1)}}(\gamma) = \Pr\left(|h_{sui}|^2 < \frac{c_j\gamma}{a_j-\gamma b_j}\right)$. Since $|h_{sui}|^2$ follows Exponential distribution, we get

$$F_{\gamma_{ui}^{(1)}}(\gamma) = \begin{cases} 0 & \text{, If } \gamma > \frac{a_j}{b_j}, \\ 1-e^{-\left(\frac{c_j\gamma}{a_j-\gamma b_j}\right)}, & \text{If } \gamma < \frac{a_j}{b_j}. \end{cases} \quad (52)$$

Consequently, the PDF of $\gamma_{ui}^{(1)}$ can be written as

$$f_{\gamma_{ui}^{(1)}}(\gamma) = \frac{a_jc_j}{(a_j-\gamma b_j)^2}e^{-\left(\frac{c_j\gamma}{a_j-\gamma b_j}\right)}, \qquad \gamma < \frac{a_j}{b_j}. \quad (53)$$

Finally, the MGF of $\gamma_{ui}^{(1)}$is

$$\mathcal{M}_{\gamma_{ui}^{(1)}}(z) = \int_0^{\frac{a_j}{b_j}} e^{-z\gamma}\frac{a_jc_j}{(a_j-\gamma b_j)^2}e^{-\left(\frac{c_j\gamma}{a_j-\gamma b_j}\right)}d\gamma. \quad (54)$$

Now, by substituting $j=2$ and $b_2=0$, we reach (18), and by substituting $j=3$ we get (21). Similarly, we derive the MGF of a general form of$\gamma_{ui}^{(2)}$which given by

$$\gamma_{ui}^{(2)} = \frac{a_j\left|\mathbf{h}_{rui}\mathbf{h}_{sr}^T\right|^2}{b_j\left|\mathbf{h}_{rui}\mathbf{h}_{sr}^T\right|^2 + c_j\left\|\mathbf{h}_{rui}\right\|^2 + d_j}, \quad (55)$$

where $j=4$ for U1 and $j=5$ for U2, and $b_4=0$. We can rewrite (55) as

$$\gamma_{ui}^{(2)} = \frac{a_j\frac{\left|\mathbf{h}_{rui}\mathbf{h}_{sr}^T\right|^2}{\left\|\mathbf{h}_{rui}\right\|^2}}{b_j\frac{\left|\mathbf{h}_{rui}\mathbf{h}_{sr}^T\right|^2}{\left\|\mathbf{h}_{rui}\right\|^2} + c_j + \frac{d_j}{\left\|\mathbf{h}_{rui}\right\|^2}} = \frac{a_j\,x}{b_j\,x + c_j + d_j\,y}, \quad (56)$$

where $x = \frac{\left|\mathbf{h}_{rui}\mathbf{h}_{sr}^T\right|^2}{\left\|\mathbf{h}_{rui}\right\|^2}$ and $y = \frac{1}{\left\|\mathbf{h}_{rui}\right\|^2}$. Hence, the CDF of $\gamma_{ui}^{(2)}$can be found as

$$F_{\gamma_{ui}^{(2)}}(\gamma) = \Pr\left(\frac{a_j\, x}{b_j\, x + c_j + d_j\, y} < \gamma\right)$$

$$= \Pr\left(x < \frac{(c_j + \phi_j)\,\gamma}{a_j - b_j\gamma}\right), \tag{57}$$

where $\phi = d_j\, y$, by condition on ϕ and since x has Exponential distribution [17],we can write the conditional CDF as $F_{\gamma_{ui}^{(2)}}(\gamma\,|\phi) = 1 - e^{-\left(\frac{(c_j+\phi)\gamma}{a_j - b_j\gamma}\right)}, \quad \gamma < \frac{a_j}{b_j}$. Now, the CDF of $\gamma_{ui}^{(2)}$can be expressed as

$$F_{\gamma_{ui}^{(2)}}(\gamma) = 1 - \int_0^\infty e^{-\left(\frac{(c_j+\phi)\gamma}{a_j - b_j\gamma}\right)} f(\phi)\, d\phi, \tag{58}$$

$$= 1 - \int_0^\infty e^{-c_j\xi} e^{-\phi\xi} f(\phi)\, d\phi = 1 - \mathcal{M}_{c_j+\phi}(\xi), \tag{59}$$

where $\xi = \frac{\gamma}{a_j - b_j\gamma}$. Therefore, the MGF of a general form of $\gamma_{ui}^{(2)}$can be derived as $\mathcal{M}_{\gamma_{ui}^{(2)}}(z) = \int_0^\infty e^{-z\gamma} f_{\gamma_{ui}^{(2)}}(\gamma)\, d\gamma$. Using integration by parts, we can get $\mathcal{M}_{\gamma_{ui}^{(2)}}(z) = 1 - z\int_0^{\frac{a_j}{b_j}} e^{-z\gamma}\, \mathcal{M}_{c_j+\phi}(\xi)\, d\gamma$, where $\mathcal{M}_{c_j+\phi}(\xi) = e^{-\xi c_j}\frac{2(d_j\xi)^{\frac{N_r}{2}} K_{N_r}\left(2\sqrt{d_j\xi}\right)}{\Gamma(N_r)}$, by substituting the values of the constants we can find the MGFs of $\gamma_{u1}^{(2)}$and $\gamma_{u2}^{(2)}$ as in (19) and (22) respectively.

Appendix B

In this appendix we derive the average sum-rate expression presented in Theorems 2 and 3. Firstly, it was presented in [53] that for any random variables $u, v > 0$

$$\mathbb{E}\left[\ln\left(1 + \frac{u}{v}\right)\right] = \int_0^\infty \frac{1}{z}\left(\mathcal{M}_v(z) - \mathcal{M}_{v+u}(z)\right) dz, \tag{60}$$

where $\mathcal{M}_v(z)$ denotes the MGF of v. Again, as in Appendix A, we will make the derivation in general form, and by substituting $\psi_1 = 0$ we can find proof of Theorem 2, and by setting $\psi_1 = 1$ for the proof for Theorem 3. To start with, we formulate the first average term in (28) as

$$\mathbb{E}\left[\log_2\left(1 + \gamma_{x_i\to r}\right)\right] = \mathbb{E}\left[\log_2\left(1 + \frac{a_j\left\|\mathbf{h}_{sr}^T\right\|^2}{b_j\left\|\mathbf{h}_{sr}^T\right\|^2 + c_j}\right)\right], \tag{61}$$

where $j = 6$ for x_2, $\gamma_{x_2\to r} = \frac{a_6\left\|\mathbf{h}_{sr}^T\right\|^2}{b_6\left\|\mathbf{h}_{sr}^T\right\|^2 + c_6}$, and $j = 7$ for $x_1$and $b_7 = 0$, $c_7 = 1$, $\gamma_{x_1\to r} = a_7\left\|\mathbf{h}_{sr}^T\right\|^2$. We set $v = b_j\left\|\mathbf{h}_{sr}^T\right\|^2 + c_j$ and $u = a_j\left\|\mathbf{h}_{sr}^T\right\|^2$. Since $\left\|\mathbf{h}_{sr}^T\right\|^2$ has Gamma distribution, $\mathcal{M}_v(z) = e^{-zc_j}(1 + b_j z)^{-N_r}$ and $\mathcal{M}_{u+v}(z) = e^{-zc_j}(1 + (a_j + b_j)\, z)^{-N_r}$. Now using (60) one can yield

$$\mathbb{E}\left[\log_2\left(1 + \frac{a_j\left\|\mathbf{h}_{sr}^T\right\|^2}{b_j\left\|\mathbf{h}_{sr}^T\right\|^2 + c_j}\right)\right] = \int_0^\infty \frac{e^{-zc_j}}{z\,\ln 2}$$

$$\times\left((1 + b_j z)^{-N_r} - (1 + (a_j + b_j)\, z)^{-N_r}\right) dz \tag{62}$$

Substituting the values of a_j, b_j and c_j we can get

$$\mathbb{E}\left[\log_2(1 + \gamma_{x_2\to r})\right] = \int_0^\infty \frac{e^{-zc_6}}{z\,\ln 2}$$

$$\times\left((1 + b_6 z)^{-N_r} - (1 + (a_6 + b_6)\, z)^{-N_r}\right) dz, \tag{63}$$

$$\mathbb{E}\left[\log_2(1 + \gamma_{x_1\to r})\right] = \int_0^\infty \frac{1}{z\,\ln 2}\left(1 - (1 + a_7 z)^{-N_r}\right) e^{-z} dz. \tag{64}$$

which can be found in closed form. Secondly, the average term, $\mathbb{E}\left[\log_2\left(1 + \gamma_{ui}^{(1)} + \gamma_{ui}^{(2)}\right)\right]$, can be found using (50) as

$$\mathbb{E}\left[\log_2\left(1 + \gamma_{ui}^{(1)} + \gamma_{ui}^{(2)}\right)\right] =$$

$$\frac{1}{\ln(2)}\int_0^\infty \frac{1}{z}\left(1 - \mathcal{M}_{\gamma_{ui}^{(1)}}(z)\,\mathcal{M}_{\gamma_{ui}^{(2)}}(z)\right) e^{-z} dz, \tag{65}$$

where $\mathcal{M}_{\gamma_{u1}^{(1)}}(z)$ and $\mathcal{M}_{\gamma_{u2}^{(1)}}(z)$ was derived in Appendix A. Now, to derive $\mathcal{M}_{\gamma_{ui}^{(2)}}(z)$, we write a general form of SINRs at the users as $\gamma_{ui}^{(2)} = \frac{a_j\|\mathbf{h}_{rui}\|^2}{b_j\|\mathbf{h}_{rui}\|^2 + c_j}$, where $j = 9$ for U1, $\gamma_{u1}^{(2)} = \frac{a_9\left\|\mathbf{h}_{ru1}\right\|^2}{b_9\left\|\mathbf{h}_{ru1}\right\|^2 + c_9}$, and $j = 10$ for U2 and $\gamma_{u2}^{(2)} = \frac{a_{10}\left\|\mathbf{h}_{ru2}\right\|^2}{b_{10}\left\|\mathbf{h}_{ru2}\right\|^2 + c_{10}}$. To find the MGF $\mathcal{M}_{\gamma_{ui}^{(2)}}(z)$, we first derive the CDF and from that, obtain the PDF. The CDF of $\gamma_{ui}^{(2)}$ can be found as

$$F_{\gamma_{ui}^{(2)}}(\gamma) = \frac{\Xi\left(N_r, \frac{c_j\gamma}{a_j - b_j\gamma}\right)}{\Gamma(N_r)},\ \gamma < \frac{a_j}{b_j}, \tag{66}$$

where $\Xi(.)$ is incomplete gamma function [45] and $\Gamma(.)$ is gamma function [45]. Therefore, the PDF of $\gamma_{ui}^{(2)}$ can be written as,

$$f_{\gamma_{ui}^{(2)}}(\gamma) =$$

$$\frac{e^{-\frac{c_j\gamma}{a_j - b_j\gamma}}\left(\frac{c_j\gamma}{a_j - b_j\gamma}\right)^{N_r - 1}\left(\frac{b_j c_j\gamma}{(a_j - b_j\gamma)^2} + \frac{c_j}{a_j - b_j\gamma}\right)}{\Gamma(N_r)}, \gamma < \frac{a_j}{b_j}. \tag{67}$$

Finally, the MGF $\mathcal{M}_{\gamma_{ui}^{(2)}}(z)$ in DF mode, can be found by $\mathcal{M}_{\gamma_{ui}^{(2)}}(z)=\int_0^{\frac{a_j}{b_j}} e^{-z\gamma} f_{\gamma_{ui}^{(2)}}(\gamma)\,d\gamma$. In case of $\psi_1=0$ $b_9=0$ and $\mathcal{M}_{\gamma_{u1}^{(2)}}(z)=\left(1+\frac{a_9}{c_9}z\right)^{-Nr}$, $\mathcal{M}_{\gamma_{u2}^{(2)}}(z)=\frac{1}{\Gamma(N_r)}\int_0^{\frac{a_{10}}{b_{10}}} e^{-\gamma\left(z+\frac{c_{10}}{a_{10}-b_{10}\gamma}\right)}$ $\times\left(\frac{c_{10}\gamma}{a_{10}-b_{10}\gamma}\right)^{N_r-1}\left(\frac{b_{10}c_{10}\gamma}{(a_{10}-b_{10}\gamma)^2}+\frac{c_{10}}{a_{10}-b_{10}\gamma}\right)d\gamma$.

In case of $\psi_1=1$ $b_{10}=0$ and $\mathcal{M}_{\gamma_{u1}^{(2)}}(z)=\int_0^{\frac{a_9}{b_9}}\frac{e^{-\gamma\left(z+\frac{c_9}{a_9-b_9\gamma}\right)}\left(\frac{c_9\gamma}{a_9-b_9\gamma}\right)^{N_r-1}\left(\frac{b_9c_9\gamma}{(a_9-b_9\gamma)^2}+\frac{c_9}{a_9-b_9\gamma}\right)}{\Gamma(N_r)}d\gamma$, $\mathcal{M}_{\gamma_{u2}^{(2)}}(z)=\left(1+\frac{a_{10}}{c_{10}}z\right)^{-N_r}$. Thirdly,

$$\mathbb{E}\left[\log_2\left(1+\gamma_{x_{\bar{i}}\to ui}^{(2)}\right)\right]=$$

$$\mathbb{E}\left[\log_2\left(1+\frac{a_8\left\|\mathbf{h}_{rui}\right\|^2}{b_8\left\|\mathbf{h}_{rui}\right\|^2+c_8}\right)\right]. \tag{68}$$

Assume $v=b_8\left\|\mathbf{h}_{rui}\right\|^2+c_8$ and $u=a_8\left\|\mathbf{h}_{rui}\right\|^2$. Since $\left\|\mathbf{h}_{rui}\right\|^2$ has Gamma distribution, $\mathcal{M}_v(z)=e^{-zc_8}(1+b_8z)^{-N_r}$ and $\mathcal{M}_{u+v}(z)=e^{-zc_8}(1+(a_8+b_8)z)^{-N_r}$. Now by using (60) we obtain

$$\mathbb{E}\left[\log_2\left(1+\gamma_{x_{\bar{i}}\to ui}^{(2)}\right)\right]=\int_0^{\infty}\frac{1}{z\,\ln 2}$$

$$\times\left((1+b_8z)^{-N_r}-(1+(a_8+b_8)z)^{-N_r}\right)e^{-zc_8}dz. \tag{69}$$

Similarly since $|h_{su1}|^2$ has Exponential distribution, we can easily find,

$$\mathbb{E}\left[\log_2\left(1+\gamma_{x_2\to u1}^{(1)}\right)\right]=$$

$$\mathbb{E}\left[\log_2\left(1+\frac{a_1|h_{su1}|^2}{b_1|h_{su1}|^2+c_1}\right)\right], \tag{70}$$

$$=\int_0^{\infty}\frac{1}{z\,\ln 2}\left(\frac{1}{1+b_1z}-\frac{1}{1+(a_1+b_1)z}\right)e^{-zc_1}dz. \tag{71}$$

APPENDIX C

This appendix derives the average secrecy rate expression in Theorem 4.

- The average Rate at U2: To begin with, it is more convenient to rewrite (13) according to

$$\gamma_{u2}^{(2)}=\frac{a_5\frac{\left|\mathbf{h}_{ru2}\mathbf{h}_{sr}^T\right|^2}{\left\|\mathbf{h}_{ru2}\right\|^2}}{b_5\frac{\left|\mathbf{h}_{ru2}\mathbf{h}_{sr}^T\right|^2}{\left\|\mathbf{h}_{ru2}\right\|^2}+c_5+\frac{d_5}{\left\|\mathbf{h}_{ru2}\right\|^2}}=\frac{u}{v}, \tag{72}$$

where $u=a_5\frac{\left|\mathbf{h}_{ru2}\mathbf{h}_{sr}^T\right|^2}{\left\|\mathbf{h}_{ru2}\right\|^2}$ and $v=b_5\frac{\left|\mathbf{h}_{ru2}\mathbf{h}_{sr}^T\right|^2}{\left\|\mathbf{h}_{ru2}\right\|^2}+c_5+\frac{d_5}{\left\|\mathbf{h}_{ru2}\right\|^2}$. Consequently, we get $\mathbb{E}(R_{u2})=\frac{1}{2}\mathbb{E}\left[\log_2\left(1+\frac{u}{v}\right)\right]$. Since $\frac{\left|\mathbf{h}_{ru2}\mathbf{h}_{sr}^T\right|^2}{\left\|\mathbf{h}_{ru2}\right\|^2}$ has Exponential distribution and $\left\|\mathbf{h}_{ru2}\right\|^2$ has Gamma distribution [17], the MGFs of u and $u+v$ in are

$$\mathcal{M}_v(z)=e^{-zc_5}\left(\frac{1}{1+b_5z}\right)\left(\frac{2\left(d_5z\right)^{\frac{N_r}{2}}}{\Gamma(N_r)}\mathrm{J}\left(N_r,2\sqrt{d_5z}\right)\right), \tag{73}$$

and

$$\mathcal{M}_{u+v}(z)=e^{-zc_5}\left(\frac{1}{1+(a_5+b_5)z}\right)$$

$$\times\left(\frac{2\left(d_5z\right)^{\frac{N_r}{2}}}{\Gamma(N_r)}\mathrm{J}\left(N_r,2\sqrt{d_5z}\right)\right). \tag{74}$$

.

By substituting $\mathcal{M}_v(z)$ and $\mathcal{M}_{u+v}(z)$ equations in (60) we can obtain the average rate at U2.

- The average Rate at the Relay: Similarly, we now calculate the average rate at the relay by first simplifying (39) as in (75), (76) and (77), where $u=\varrho_{11}\frac{\left\|\mathbf{h}_{sr}^T\right\|^2}{\left\|\mathbf{h}_{u1r}^T\right\|^2}$ and $v=\frac{1}{\left\|\mathbf{h}_{u1r}^T\right\|^2}\left(a_{11}\left\|\mathbf{h}_{sr}^T\right\|^2+r_{11}\right)+b_{11}\left|\overline{h_{su1}}\right|^2+\left\|\overline{\mathbf{h}_{ru1}}\right\|^2c_{11}$. To calculate the average rate at the relay using (60), we derive $\mathcal{M}_v(z)$ and $\mathcal{M}_{u+v}(z)$ in this case as follows. First, let $K=\frac{1}{\left\|\mathbf{h}_{u1r}^T\right\|^2}\left(a_{11}\left\|\mathbf{h}_{sr}^T\right\|^2+r_{11}\right)$, $L=b_{11}\left|\overline{h_{su1}}\right|^2$, and $\Theta=\left\|\overline{\mathbf{h}_{ru1}}\right\|^2c_{11}$. Given that $\left\|\mathbf{h}_{sr}^T\right\|^2$ follows Gamma distribution, the $\mathcal{M}_K(z)$ can be obtained by condition on $\left\|\mathbf{h}_{u1r}^T\right\|^2$ as $\mathcal{M}_K(z\,|x\,)=e^{-r_{11}zx}(1+a_{11}xz)^{-N_r}$. Consequently,

$$\mathcal{M}_K(z)=\int_0^{\infty}\frac{e^{-r_{11}zx}}{\Gamma(N_r)}(1+a_{11}xz)^{-N_r}x^{(-N_r-1)}e^{-\frac{1}{x}}dx. \tag{78}$$

Since $\left|\overline{h_{su1}}\right|^2$ has Exponential distribution, $\mathcal{M}_L(z)=\frac{1}{1+b_{11}z}$. Since $\left\|\overline{\mathbf{h}_{ru1}}\right\|^2$ has Gamma distribution, the MGF $\mathcal{M}_\Theta(z)$ can be easily obtained as, $\mathcal{M}_\Theta(z)=(1+c_{11}z)^{-N_r}$. Consequently, the MGF of v is $\mathcal{M}_v(z)=\mathcal{M}_K(z)\mathcal{M}_L(z)\mathcal{M}_\Theta(z)$, and the MGF of $u+v$ can be directly obtained as $\mathcal{M}_{u+v}(z)=\mathcal{M}_W(z)\mathcal{M}_L(z)\mathcal{M}_\Theta(z)$where $W=K+u$ and,

$$\mathcal{M}_W(z)=\int_0^{\infty}\frac{e^{-r_{11}zx}}{\Gamma(N_r)}$$

$$\times(1+(a_{11}+\varrho_{11})xz)^{-N_r}x^{(-N_r-1)}e^{-\frac{1}{x}}dx. \tag{79}$$

Finally, by substituting $\mathcal{M}_v(z)$ and $\mathcal{M}_{u+v}(z)$into (60), we can find the average rate at the relay.

$$\gamma_{x_2\to r}=\frac{\varrho_{11}\left\|\mathbf{h}_{sr}^{T}\right\|^{2}}{a_{11}\left\|\mathbf{h}_{sr}^{T}\right\|^{2}+\left\|\mathbf{h}_{u1r}^{T}\right\|^{2}\left(b_{11}\left|\overline{h_{su1}}\right|^{2}+c_{11}\left\|\overline{\mathbf{h}_{ru1}}\right\|^{2}\right)+r_{11}}, \tag{75}$$

$$=\frac{\varrho_{11}\frac{\left\|\mathbf{h}_{sr}^{T}\right\|^{2}}{\left\|\mathbf{h}_{u1r}^{T}\right\|^{2}}}{a_{11}\frac{\left\|\mathbf{h}_{sr}^{T}\right\|^{2}}{\left\|\mathbf{h}_{u1r}^{T}\right\|^{2}}+b_{11}\left|\overline{h_{su1}}\right|^{2}+c_{11}\left\|\overline{\mathbf{h}_{ru1}}\right\|^{2}+\frac{r_{11}}{\left\|\mathbf{h}_{u1r}^{T}\right\|^{2}}}, \tag{76}$$

$$=\frac{\varrho_{11}\frac{\left\|\mathbf{h}_{sr}^{T}\right\|^{2}}{\left\|\mathbf{h}_{u1r}^{T}\right\|^{2}}}{\frac{1}{\left\|\mathbf{h}_{u1r}^{T}\right\|^{2}}\left(a_{11}\left\|\mathbf{h}_{sr}^{T}\right\|^{2}+r11\right)+b_{11}\left|\overline{h_{su1}}\right|^{2}+\left\|\overline{\mathbf{h}_{ru1}}\right\|^{2}c_{11}}=\frac{u}{v}, \tag{77}$$

REFERENCES

[1] Z. Ding, Y. Liu, J. Choi, Q. Sun, M. Elkashlan, C. L. I, and H. V. Poor, "Application of non-orthogonal multiple access in LTE and 5G networks," *IEEE Communications Magazine*, vol. 55, pp. 185–191, Feb. 2017.

[2] Z. Ding, Z. Yang, P. Fan, and H. V. Poor, "On the performance of non-orthogonal multiple access in 5G systems with randomly deployed users," *IEEE Signal Processing Letters*, vol. 21, pp. 1501–1505, Dec. 2014.

[3] S. Timotheou and I. Krikidis, "Fairness for non-orthogonal multiple access in 5G systems," *IEEE Signal Processing Letters*, vol. 22, pp. 1647–1651, Oct. 2015.

[4] Z. Yang, Z. Ding, P. Fan, and G. K. Karagiannidis, "On the performance of non-orthogonal multiple access systems with partial channel information," *IEEE Transactions on Communications*, vol. 64, pp. 654–667, Feb. 2016.

[5] Z. Ding, P. Fan, and H. V. Poor, "Impact of user pairing on 5G non-orthogonal multiple-access downlink transmissions," *IEEE Transactions on Vehicular Technology*, vol. 65, pp. 6010–6023, Aug. 2016.

[6] J. B. Kim and I. H. Lee, "Non-orthogonal multiple access in coordinated direct and relay transmission," *IEEE Communications Letters*, vol. 19, pp. 2037–2040, Nov. 2015.

[7] J. Men and J. Ge, "Non-orthogonal multiple access for multiple-antenna relaying networks," *IEEE Communications Letters*, vol. 19, pp. 1686–1689, Oct. 2015.

[8] J. B. Kim and I. H. Lee, "Capacity analysis of cooperative relaying systems using non-orthogonal multiple access," *IEEE Communications Letters*, vol. 19, pp. 1949–1952, Nov. 2015.

[9] R. Jiao, L. Dai, J. Zhang, R. MacKenzie, and M. Hao, "On the performance of NOMA-based cooperative relaying systems over Rician fading channels," *IEEE Transactions on Vehicular Technology*, vol. 66, pp. 11409–11413, Dec. 2017.

[10] Y. Liu, Z. Ding, M. Elkashlan, and H. V. Poor, "Cooperative non-orthogonal multiple access with simultaneous wireless information and power transfer," *IEEE Journal on Selected Areas in Communications*, vol. 34, pp. 938–953, April. 2016.

[11] N. T. Do, D. B. D. Costa, T. Q. Duong, and B. An, "A BNBF user selection scheme for NOMA-based cooperative relaying systems with SWIPT," *IEEE Communications Letters*, vol. 21, pp. 664–667, March. 2017.

[12] Z. Yang, Z. Ding, P. Fan, and N. Al-Dhahir, "The impact of power allocation on cooperative non-orthogonal multiple access networks with SWIPT," *IEEE Transactions on Wireless Communications*, vol. 16, pp. 4332–4343, July. 2017.

[13] N. Pappas, M. Kountouris, J. Jeon, A. Ephremides, and A. Traganitis, "Effect of energy harvesting on stable throughput in cooperative relay systems," *Journal of Communications and Networks*, vol. 18, pp. 261–269, Apr. 2016.

[14] N. Pappas, J. Jeon, A. Ephremides, and A. Traganitis, "Optimal utilization of a cognitive shared channel with a rechargeable primary source node," *Journal of Communications and Networks*, vol. 14, pp. 162–168, Apr. 2012.

[15] A. Wyner, "The wire-tap channel," *Bell Syst. Tech. J.*, vol. 54, pp. 1355–1387, Oct. 1975.

[16] S. Goel and R. Negi, "Guaranteeing secrecy using artificial noise," *IEEE Transactions on Wireless Communications*, vol. 7, pp. 2180–2189, Jun. 2008.

[17] A. Salem, K. A. Hamdi, and K. M. Rabie, "Physical layer security with RF energy harvesting in AF multi-antenna relaying networks," *IEEE Transactions on Communications*, vol. 64, pp. 3025–3038, Jul. 2016.

[18] Y. Oohama, "Capacity theorems for relay channels with confidential messages," in *proc. Information Theory, 2007. ISIT 2007. IEEE International Symposium on*, pp. 926–930, Jun. 2007.

[19] X. He and A. Yener, "Cooperation with an untrusted relay: A secrecy perspective," *IEEE Transactions on Information Theory*, vol. 56, pp. 3807–3827, Aug. 2010.

[20] X. He and A. Yener, "The role of an untrusted relay in secret communication," in *proc. Information Theory, 2008. ISIT 2008. IEEE International Symposium on*, pp. 2212–2216, Jul. 2008.

[21] S. S. Kalamkar and A. Banerjee, "Secure communication via a wireless energy harvesting untrusted relay," *IEEE Transactions on Vehicular Technology*, vol. 66, pp. 2199–2213, Mar. 2017.

[22] J. Xiong, L. Cheng, D. Ma, and J. Wei, "Destination-aided cooperative jamming for dual-hop amplify-and-forward MIMO untrusted relay systems," *IEEE Transactions on Vehicular Technology*, vol. 65, pp. 7274–7284, Sept. 2016.

[23] L. Zhang, J. Liu, M. Xiao, G. Wu, Y. C. Liang, and S. Li, "Performance analysis and optimization in downlink NOMA systems with cooperative full-duplex relaying," *IEEE Journal on Selected Areas in Communications*, vol. 35, pp. 2398–2412, Oct. 2017.

[24] Z. Ding, P. Fan, and H. V. Poor, "Impact of user pairing on 5G nonorthogonal multiple-access downlink transmissions," *IEEE Transactions on Vehicular Technology*, vol. 65, pp. 6010–6023, Aug. 2016.

[25] J. Huang, A. Mukherjee, and A. L. Swindlehurst, "Secure communication via an untrusted non-regenerative relay in fading channels," *IEEE Transactions on Signal Processing*, vol. 61, pp. 2536–2550, May. 2013.

[26] X. Chen, L. Lei, H. Zhang, and C. Yuen, "Large-scale MIMO relaying techniques for physical layer security: AF or DF?," *IEEE Transactions on Wireless Communications*, vol. 14, pp. 5135–5146, Sept. 2015.

[27] R. Zhao, Y. Huang, W. Wang, and V. K. N. Lau, "Ergodic achievable secrecy rate of multiple-antenna relay systems with cooperative jamming," *IEEE Transactions on Wireless Communications*, vol. 15, pp. 2537–2551, Apr. 2016.

[28] I. Krikidis, S. Sasaki, S. Timotheou, and Z. Ding, "A low complexity antenna switching for joint wireless information and energy transfer in MIMO relay channels," *IEEE Transactions on Communications*, vol. 62, pp. 1577–1587, May. 2014.

[29] Z. Ding, X. Lei, G. K. Karagiannidis, R. Schober, J. Yuan, and V. K. Bhargava, "A survey on non-orthogonal multiple access for 5G networks: Research challenges and future trends," *IEEE Journal on Selected Areas in Communications*, vol. 35, pp. 2181–2195, Oct. 2017.

[30] Z. Shi, S. Ma, H. ElSawy, G. Yang, and M. Alouini, "Cooperative HARQ-assisted NOMA scheme in large-scale D2D networks," *IEEE Transactions on Communications*, vol. 66, pp. 4286–4302, Sep. 2018.

[31] Y. Liu, Z. Ding, M. Elkashlan, and H. V. Poor, "Cooperative non-orthogonal multiple access with simultaneous wireless information and power transfer," *IEEE Journal on Selected Areas in Communications*, vol. 34, pp. 938–953, Apr. 2016.

[32] Z. Ding, R. Schober, and H. V. Poor, "A general MIMO framework for NOMA downlink and uplink transmission based on signal alignment," *IEEE Transactions on Wireless Communications*, vol. 15, pp. 4438–4454, Jun. 2016.

[33] H. Chingoska, Z. Hadzi-Velkov, I. Nikoloska, and N. Zlatanov, "Resource allocation in wireless powered communication networks with non-orthogonal multiple access," *IEEE Wireless Communications Letters*, vol. 5, pp. 684–687, Dec. 2016.

[34] W. J. H. Y.W. Peter Hong and J. Kuo, *Cooperative Communications and Networking*. 2010: Springer.

[35] X. Bao and J. Li, "Efficient message relaying for wireless user cooperation: Decode amplify forward (DAF) and hybrid DAF and coded-cooperation," *IEEE Transactions on Wireless Communications*, vol. 6, pp. 3975–3984, Nov. 2007.

[36] T. Liu, L. Song, Y. Li, Q. Huo, and B. Jiao, "Performance analysis of hybrid relay selection in cooperative wireless systems," *IEEE Transactions on Communications*, vol. 60, pp. 779–788, Mar. 2012.

[37] Z. Bai, J. Jia, C. X. Wang, and D. Yuan, "Performance analysis of SNR-based incremental hybrid decode-amplify-forward cooperative relaying protocol," *IEEE Trans. Commun.*, vol. 63, pp. 2094–2106, Jun. 2015.

[38] M. Zamani and A. K. Khandani, "Broadcast approaches to the diamond channel," *IEEE Transactions on Information Theory*, vol. 60, pp. 623–642, Jan. 2014.

[39] Y. Feng, S. Yan, Z. Yang, N. Yang, and W. Zhu, "TAS-based incremental hybrid decode amplify forward relaying for physical layer security enhancement," *IEEE Transactions on Communications*, vol. 65, pp. 3876–3891, Sept. 2017.

[40] T. T. Duy and H. Kong, "Performance analysis of hybrid decode amplify forward incremental relaying cooperative diversity protocol using SNR-based relay selection," *Journal of Communications and Networks*, vol. 14, pp. 703–709, Dec. 2012.

[41] H. Liu, Z. Ding, K. J. Kim, K. S. Kwak, and H. V. Poor, "Decode-and-forward relaying for cooperative NOMA systems with direct links," *IEEE Transactions on Wireless Communications*, pp. 1–1, 2018.

[42] J. M. Romero-Jerez, J. P. Pena-Martin, and A. J. Goldsmith, "Outage probability of mrc with arbitrary power cochannel interferers in nakagami fading," *IEEE Transactions on Communications*, vol. 55, no. 7, pp. 1283–1286, 2007.

[43] Z. Ding, M. Peng, and H. V. Poor, "Cooperative non-orthogonal multiple access in 5G systems," *IEEE Communications Letters*, vol. 19, pp. 1462–1465, Aug. 2015.

[44] Y. Xu, C. Shen, Z. Ding, X. Sun, S. Yan, G. Zhu, and Z. Zhong, "Joint beamforming and power-splitting control in downlink cooperative SWIPT NOMA systems," *IEEE Transactions on Signal Processing*, vol. 65, pp. 4874–4886, Sep. 2017.

[45] M. Abramowitz and I. A. Stegun, *Handbook of Mathematical Functions With Formulas, Graphs, and Mathematical Tabl*. Washington, D.C.: U.S. Dept. Commerce, 1972.

[46] G. Zheng, "Joint beamforming optimization and power control for full-duplex MIMO two-way relay channel," *IEEE Transactions on Signal Processing*, vol. 63, pp. 555–566, Feb. 2015.

[47] Z. Xiang, W. Yang, G. Pan, Y. Cai, and X. Sun, "Secure transmission in non-orthogonal multiple access networks with an untrusted relay," *IEEE Wireless Communications Letters*, pp. 1–1, 2019.

[48] P. K. Gopala, L. Lai, and H. El Gamal, "On the secrecy capacity of fading channels," *IEEE Trans. Inf. Theory*, vol. 54, pp. 4687–4698, Oct. 2008.

[49] J. Li and A. P. Petropulu, "On ergodic secrecy rate for Gaussian MISO wiretap channels," *IEEE Trans. Wireless Commun.*, vol. 10, pp. 1176–1187, Apr. 2011.

[50] A. Salem and K. A. Hamdi, "Wireless power transfer in multi-pair two-way AF relaying networks," *IEEE Trans. Commun.*, vol. 64, pp. 4578–4591, Nov. 2016.

[51] H. Niu, B. Zhang, and D. Guo, "Outage constrained robust beamforming and power splitting for secure MISO SWIPT channel," *IEEE Wireless Communications Letters*, vol. 6, pp. 826–829, Dec. 2017.

[52] G. Pan, H. Lei, Y. Yuan, and Z. Ding, "Performance analysis and optimization for SWIPT wireless sensor networks," *IEEE Transactions on Communications*, vol. 65, pp. 2291–2302, May. 2017.

[53] K. Hamdi, "A useful lemma for capacity analysis of fading interference channels," *IEEE Trans. Commun.*, vol. 58, pp. 411–416, Feb. 2010.